STAR Protocols

CellPress
OPEN ACCESS

Protocol

Real-time visualization of exo- and endocytosis membrane dynamics with confocal and super-resolution microscopy

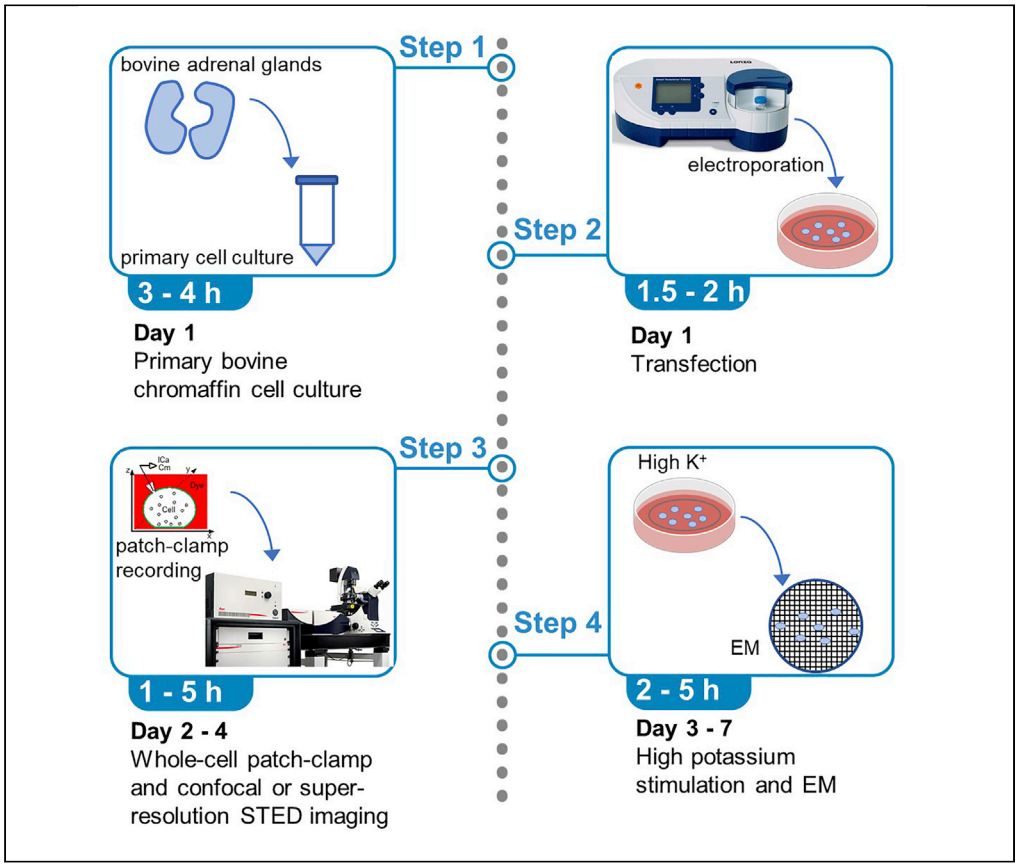

Real-time confocal and super-resolution imaging reveals membrane dynamics of exo- and endocytosis, including hemi-fusion, fusion pore opening, expansion, constriction, closure (kiss-and-run), fused-vesicle shrinking (shrink fusion), and flat membrane transition to vesicles via intermediate Λ- and Ω-shape structures. Here, we describe a protocol for imaging these membrane dynamics, including primary culture of bovine adrenal chromaffin cells, fluorescent probe application, patch-clamp to deliver depolarization and evoke exo- and endocytosis, electron microscopy (EM), and real-time confocal and stimulated emission depletion (STED) microscopy.

Publisher's note: Undertaking any experimental protocol requires adherence to local institutional guidelines for laboratory safety and ethics.

Xiaoli Guo, Sue Han, Lisi Wei, Gianvito Arpino, Wonchul Shin, Xin Wang, Ling-Gang Wu

sue.han@nih.gov (S.H.)
wul@ninds.nih.gov (L.-G.W.)

Highlights

Real-time visualization of membrane dynamics of vesicle fusion and endocytosis

Confocal imaging, STED imaging, and electron microscopy of exo-endocytosis

Fluorescent probes and procedures for labeling plasma membrane and vesicles

Detailed protocol for culturing chromaffin cells from bovine adrenal gland

Guo et al., STAR Protocols 3, 101404
June 17, 2022
https://doi.org/10.1016/j.xpro.2022.101404

STAR Protocols

CellPress
OPEN ACCESS

Protocol

Real-time visualization of exo- and endocytosis membrane dynamics with confocal and super-resolution microscopy

Xiaoli Guo,[1,2] Sue Han,[1,2,4,*] Lisi Wei,[1] Gianvito Arpino,[1,3] Wonchul Shin,[1] Xin Wang,[1] and Ling-Gang Wu[1,5,*]

[1]National Institute of Neurological Disorders and Stroke, Bethesda, MD 20892, USA

[2]These authors contributed equally

[3]Present address: Emme 3 Srl, Via Luigi Meraviglia, 31, 20020 Lainate, MI, Italy

[4]Technical contact

[5]Lead contact

*Correspondence: sue.han@nih.gov (S.H.), wul@ninds.nih.gov (L.-G.W.)
https://doi.org/10.1016/j.xpro.2022.101404

SUMMARY

Real-time confocal and super-resolution imaging reveals membrane dynamics of exo- and endocytosis, including hemi-fusion, fusion pore opening, expansion, constriction, closure (kiss-and-run), fused-vesicle shrinking (shrink fusion), and flat membrane transition to vesicles via intermediate Λ- and Ω-shape structures. Here, we describe a protocol for imaging these membrane dynamics, including primary culture of bovine adrenal chromaffin cells, fluorescent probe application, patch-clamp to deliver depolarization and evoke exo- and endocytosis, electron microscopy (EM), and real-time confocal and stimulated emission depletion (STED) microscopy.

For complete details on the use and execution of this protocol, please refer to Zhao et al. (2016), Shin et al. (2018), and Shin et al. (2021).

BEFORE YOU BEGIN

Vesicle fusion and endocytosis mediate fundamental biological functions, such as exocytosis, intracellular trafficking, synaptic transmission, and viral infection (Gan and Watanabe, 2018; Jackson and Chapman, 2008; Kavalali and Jorgensen, 2014; Kononenko and Haucke, 2015; Sharma and Lindau, 2018; Wu et al., 2014a). Vesicle fusion involves fusion pore opening and merging of the fusing vesicle at the fusing site of the membrane, whereas endocytosis must involve transformation of flat membrane into oval/round vesicles. These membrane dynamics are traditionally studied with electron microscopy (EM), which does not provide real-time dynamics (Ceccarelli et al., 1972; He et al., 2009; Heuser and Reese, 1973, 1981; Kononenko et al., 2014; Miller and Heuser, 1984; Watanabe et al., 2013; Wu et al., 2014b, 2016). Many fluorescence imaging studies had attempted to resolve some of these membrane dynamics, particularly the pore behavior, indirectly (Abbineni et al., 2018; Anantharam et al., 2011; Betz et al., 1992; Bhat and Thorn, 2009; Sankaranarayanan and Ryan, 2000; Taraska et al., 2003; Zhang et al., 2009). Electrophysiological methods have also been used to detect pore behaviors rapidly, but indirectly (Albillos et al., 1997; He et al., 2006; Klyachko and Jackson, 2002; Neher and Marty, 1982; Sun and Wu, 2001; Sun et al., 2002; Von Gersdorff and Matthews, 1994; Wightman et al., 1991). Recent studies in live bovine adrenal chromaffin cells have managed to visualize the membrane dynamics of vesicle fusion and endocytosis in real-time, leading to discovery of fusion pore dynamics, fusion modes, and endocytic mechanisms (Chiang et al., 2014; Ge et al., 2021; Shin et al., 2018, 2020, 2021; Wen et al., 2016; Zhao et al., 2016).

Here, we present an experimental protocol of procedures, reagents and equipment required for real-time visualization of the membrane dynamics of vesicle fusion and endocytosis in chromaffin cells. We describe the procedure for confocal microscopy, super-resolution STED microscopy, EM, as well as the procedure for primary culture of bovine adrenal chromaffin cells. Membrane dynamics of vesicle fusion described here include direct observation of three fusion modes: 1) close-fusion (also called kiss-and-run), involving fusion pore opening and closure, 2) stay-fusion, involving fusion pore opening and maintenance of an opened pore, and 3) shrink-fusion, involving shrinkage of the fusion-generated Ω-shape profile until it merges completely with the plasma membrane (Chiang et al., 2014; Shin et al., 2018, 2020). Membrane dynamics of endocytosis described here include direct observation of the flat-to-round transformation and pore closure of the preformed Ω-shape membrane profile, the latter of which is a major driving force mediating various forms of endocytosis (Shin et al., 2021). We also described the protocol for electron microscopy of membrane profiles after chemical fixation.

Institutional permissions

The procedures involving animal use followed the guidelines of National Institute of Health (NIH) and were approved by the Animal Care and Use Committee at NIH.

Obtain bovine adrenal glands

Timing: 1–3 h

1. Collect 8–10 fresh adult (21–27 months old) male bovine adrenal glands from a local abattoir and transport the glands in a sterile 500-mL capped storage bottle containing 250 mL ice-cold Locke's solution.

   Note: Transport the bottle in a cooler containing ice.

   Note: Fresh bovine adrenal glands should be obtained for each culture.

   Note: Inform the abattoir to leave the fat on the glands, as it may provide protection against contamination.

Prepare for cell culture

Timing: 30 min

2. Transfer 25-mm diameter, #1.5 thickness, sterilized poly-D-Lysine and laminin-coated German coverslips into 35-mm TC-treated culture dishes using sterilized fine-tip forceps.
3. Pre-warm a 37°C water bath.
4. Pre-warm Locke's solution and DMEM (10% FBS) to 20°C–22°C.
5. Prepare digestion enzyme in Locke's solution when glands arrive and keep it at 20°C–22°C.

KEY RESOURCES TABLE

REAGENT or RESOURCE	SOURCE	IDENTIFIER
Biological samples		
Bovine adrenal glands	J. W. Treuth and Sons, Inc.	N/A
Chemicals, peptides, and recombinant proteins		
DMEM medium	Thermo Fisher Scientific	Cat#11885084
Fetal bovine serum	Thermo Fisher Scientific	Cat#10082147
Collagenase P	MilliporeSigma	Cat#11249002001
Trypsin inhibitor from chicken egg white	MilliporeSigma	Cat#T9253
Bovine serum albumin	MilliporeSigma	Cat#A2153

(*Continued on next page*)

Continued

REAGENT or RESOURCE	SOURCE	IDENTIFIER
Sodium chloride	MilliporeSigma	Cat#S7653
Potassium chloride	MilliporeSigma	Cat#P4504
Sodium phosphate dibasic	MilliporeSigma	Cat#S0876
Sodium phosphate monobasic	MilliporeSigma	Cat#S8282
HEPES	MilliporeSigma	Cat#H3375
D-(+)-Glucose	MilliporeSigma	Cat#G8270
Sodium hydroxide	MilliporeSigma	Cat#S8045
Tetraethylammonium chloride	MilliporeSigma	Cat#T2265
L-Glutamic acid	MilliporeSigma	Cat#49449
Ethylene glycol-bis(2-aminoethylether)-N,N,N′,N′-tetraacetic acid	MilliporeSigma	Cat#E0396
Cesium hydroxide solution	MilliporeSigma	Cat#232041
Adenosine 5′-triphosphate magnesium salt	MilliporeSigma	Cat#A9187
Guanosine 5′-triphosphate sodium salt hydrate	MilliporeSigma	Cat#G8877
Atto 488 carboxy	ATTO-TEC	Cat#AD 488-21
Atto 655 carboxy	ATTO-TEC	Cat#AD 655-21
Atto 532 carboxy	ATTO-TEC	Cat#AD 532-21
FFN511	Abcam	Cat#AB120331
Paraformaldehyde aqueous solution, 16%	Electron Microscopy Sciences	Cat#30525-89-4
Glutaraldehyde aqueous solution, 50%	Electron Microscopy Sciences	Cat#16300
Sodium cacodylate	MilliporeSigma	Cat#6131-99-3
Glycine	MilliporeSigma	Cat#56-40-6
Epon-812	Electron Microscopy Sciences	Cat#13940
Tannic acid	MilliporeSigma	Cat#1401-55-4
Uranyl acetate (powder)	Electron Microscopy Sciences	Cat#22400
Osmium tetroxide	Electron Microscopy Sciences	Cat#19110
Ultrostain I (uranyl acetate solution)	Leica	Cat#705529
Ultrostain II (lead citrate solution)	Leica	Cat#705530
Critical commercial assays		
Basic nucleofector™ kit for primary mammalian neurons	Lonza	Cat#VPI-1003
Software and algorithms		
Igor Pro	WaveMetrics	http://www.wavemetrics.com/
Pulse	HEKA Elektronik	https://www.heka.com/
Huygens professional	Scientific Volume Imaging	https://svi.nl/Huygens-Professional
Leica Application Suite X	Leica	https://www.leicabiosystems.com/
ImageJ	NIH	https://imagej.nih.gov/ij/
Other		
Leica SP5 confocal	Leica Microsystems	https://www.leica-microsystems.com/products/confocal-microscopes/p/leica-tcs-sp5/
Leica TCS SP8 STED 3×	Leica Microsystems	https://www.leica-microsystems.com/products/confocal-microscopes/p/leica-tcs-sp8-sted-one/
Nucleofector™ 2b device	Lonza	Cat#AAB-1001
Micropipette puller	Sutter Instrument	Cat#P-97
Vapro pressure osmometer	ELITechGroup	Cat#NC0044806
pH meter	WTW inoLab	Cat#WTWPH720
Capillary glass pipette	Warner Instruments	Cat#640795
Microloader	Eppendorf	Cat#930001007
35-mm TC-treated culture dish	Corning	Cat#430165
500-mL vacuum filter/storage bottle system, 0.22-μm pore	Corning	Cat#430769
Poly-D-lysine and laminin coated German coverslips	Neuvitro Corporation	Cat#GG-25-1.5-Laminin

(*Continued on next page*)

Continued

REAGENT or RESOURCE	SOURCE	IDENTIFIER
Luer-Lok tip 30-mL syringe	Fisher Scientific	Cat#302832
Millex-GP syringe filter unit, 0.22-μm	MilliporeSigma	Cat#SLGP033RB
Millex-FG syringe filter unit, 0.20-μm	MilliporeSigma	Cat#SLFGR04NL
100-μm nylon mesh	ELKO Filtering Co	Cat#03-80/37
100-μm cell strainer	Corning	Cat#352360
10-mL stripette	Corning	Cat#4488
25-mL stripette	Corning	Cat#4489
50-mL stripette	Corning	Cat#4490
Iris scissors, 11 cm, supercut	World Precision Instruments	Cat#501263-G
Metzenbaum scissors, supercut	World Precision Instruments	Cat#14214-G
Dumont tweezers	World Precision Instruments	Cat#14188
Easy-grip 500-mL bottle	MilliporeSigma	Cat#CLS430282
50-mL centrifuge tube	NEST Scientific	Cat#602072
15-mL centrifuge tube	NEST Scientific	Cat#601052

MATERIALS AND EQUIPMENT

Locke's solution

Reagent	Final concentration (mM)	Amount (g)
NaCl	145	8.465
KCl	5.4	0.403
Na_2HPO_4	2.15	0.305
NaH_2PO_4	0.85	0.102
HEPES	10	2.382
D-(+)-Glucose	5.6	1.008
ddH_2O		Add to 1 L
Total		**1 L**

Note: After adjusting PH to 7.3 with 5 M NaOH, filter the solution using a 500-mL vacuum filter/storage bottle system (0.2-μm pore) and keep it at 4°C. Make fresh Locke's solution every week.

Collagenase solution

Reagent	Final concentration (mg/mL)	Amount (mg)
Collagenase P	1.5	45
Trypsin inhibitor from chicken egg white	0.325	9.75
Bovine serum albumin	5	150
Locke's solution		Add to 30 mL
Total		**30 mL**

Note: Prepare collagenase solution with Locke's solution.

Note: Prepare fresh collagenase solution in a 50-mL conical tube immediately before starting dissection.

Note: Each gland needs ~10 mL of collagenase solution, so here 30 mL is good for 3 glands.

Bath solution for patch-clamp

Reagent	Final concentration (mM)	Amount
NaCl	125	1.826 g
HEPES	10	0.596 g
KCl	4.5	0.084 g

(*Continued on next page*)

Continued		
Reagent	Final concentration (mM)	Amount
D-(+)-Glucose	10	0.45 g
TEA chloride	20	0.826 g
$MgCl_2$ (2 M)	1	0.125 mL
$CaCl_2$ (2 M)	5	0.625 mL
Total		250 mL

Note: After adjusting pH to 7.2 with 5 M NaOH, the osmolarity should be 300 ± 10 mOsm; Filter the solution using a 500-mL vacuum filter/storage bottle system (0.22-μm pore) and keep it at 4°C up to one month.

Note: For the high potassium bath solution used in EM, adjust NaCl to 60 mM, 0.876 g and KCl to 70 mM, 1.307 g.

Recording electrode internal solution for patch-clamp		
Reagent	Final concentration (mM)	Amount
L-Glutamic acid	130	0.478 g
EGTA	0.5	4.75 mg
HEPES	30	0.179 g
NaCl	12	17.5 mg
$MgCl_2$ (2 M)	1	12.5 μL

Adjust PH to 7.2 with CsOH; then quickly add:		
ATP-Mg	2	25.36 mg
GTP-Na	0.5	6.5 mg
Total		25 mL

Note: Adjust pH to 7.2 again with CsOH.

Note: Adjust osmolarity to 308 ± 5 mOsm with 130 mM L-Glutamic acid.

Note: Prepare internal solution on ice, aliquot it in 1.5-mL micro-centrifuge tubes and store it at −20°C for at least one month or −80°C for at least several months.

Note: Filter pipette solution using Millex-FG 0.2-μm syringe filter just before doing patch-clamp recording and keep it on ice during the experiment.

Complete culture medium		
Reagent	Final concentration (%)	Amount (mL)
DMEM	90	450 mL
FBS	10	50 mL
Total		500 mL

Note: The pH of the medium is critical for cell culture. After preparation, immediately aliquot the medium into 50-mL conical tubes and sealed the tube with parafilm. Check the color of the medium before use. Make fresh medium every week or every two weeks.

0.2 M sodium cacodylate buffer		
Reagent	Final concentration (M)	Amount
Sodium cacodylate	0.2	2.76 g
Total		**100 mL**

Note: Adjust PH to 7.4 with HCl.

Note: This solution can be stored at 4°C for several months.

2% glutaraldehyde/2% paraformaldehyde fixative solution		
Reagent	Final concentration	Amount
16% PFA	2%	6.25 mL
50% Glutaraldehyde	2%	2 mL
0.2 M sodium cacodylate buffer	0.1 M	25 mL
Total		**50 mL**

Note: This solution should be prepared fresh.

2% glutaraldehyde/2% paraformaldehyde/4% tannic acid fixative solution		
Reagent	Final concentration	Amount
16% PFA	2%	6.25 mL
50% Glutaraldehyde	2%	2 mL
tannic acid	4%	2 g
0.2 M sodium cacodylate buffer	0.1 M	25 mL
Total		**50 mL**

Note: Add tannic acid in the hood, add a stir bar, and mix them at a slow speed. The pH is adjusted to pH 7.4 with 3 M NaOH.

Note: Filter the amount needed for your experiment. Use a large nitrocellulose filter and a syringe draining into a Falcon tube. Put it on ice to cool.

Note: This solution should be prepared fresh.

STEP-BY-STEP METHOD DETAILS

Primary culture of bovine adrenal chromaffin cells – day 1

Timing: 3–4 h

The procedure described below is intended for two or three glands. Sterilize and inject Locke's solution and collagenase solution into the adrenal glands with a 0.22-μm syringe filter attached to a 30-mL syringe. Exercise care when performing the injections as the glands may rupture with excessive pressure. All the procedures below are performed in a cell culture hood.

1. Tissue Dissection.
   a. Unfold autoclaved surgical pack I (Figure 1A).
   b. Choose only intact glands and discard those with visible signs of internal blood coagulation. Smaller glands normally yield cells with better release activity (Figure 1B).
   c. Remove the surrounding fat and connective tissue from the glands. Try to remove as much fat as possible. Also remove the fat and connective tissue surrounding the adrenal vein (Figure 1C).
2. Place the glands in a sterile petri dish for adrenal glands cleaning. To remove blood, inject each gland from the adrenal vein 10–20 times with 1.5–3 mL Locke's solution at 20°C–22°C (Figure 1D).

   Note: When injecting Locke's solution into the glands, you should feel it swell slightly.

   Note: It is essential to remove all blood when washing the glands.

3. Wash the glands with 2–3 mL collagenase solution to get rid of the Locke's solution remaining in the glands. Hold the syringe and maintain constant pressure for a few seconds to keep the collagenase solution in the end of the adrenal vein.
4. Inject the glands with 2–3 mL collagenase solution and maintain constant syringe pressure for a few seconds to ensure the collagenase solution reaches the end of the adrenal vein. Place the glands in a glass beaker. Cover the beaker with foil and incubate for 10 min in the 37°C water bath (Figure 1E).
5. After 10 min, inject another 1–2 mL collagenase solution into the adrenal vein. It is not necessary to maintain constant syringe pressure for the second injection, as the gland is partially digested, and the collagenase solution will get into the vein easily. Cover the beaker with foil and incubate for another 10 min in the water bath.

   Note: Use less collagenase solution for the second injection to avoid over-digestion and rupture of the glands.

6. After 10 min, take the glass beaker out of the water bath. The glands should be noticeably softer, indicating success of the digestion.
7. Unfold autoclaved surgical pack II (Figure 1A) and open the gland longitudinally (along its length) using a sterile scissor. It should appear with the cream-colored section representing the medulla (Figure 1F). Use curved fine forceps to collect the medulla material and transfer it to a clean petri dish containing 50 mL Locke's solution (Figures 1F–1H). Do not collect any red or purple material that contains cortical cells.
8. Using a sterilized small scissor, cut the medulla tissue into small pieces (Figure 1I).
9. Triturate the material 5–10 times with a 50-mL stripette (Figure 1J). Pass the dissociated material into a beaker through an 80–100 μm sterilized nylon mesh to remove the bulk debris (Figure 1K). Collect the cells in a 50-mL conical tube.
10. Centrifuge at 48 × *g* for 3 min; discard the supernatant. Resuspend the pellet in 20 mL Locke's solution and triturate it with a stripette 5–10 times.
11. Pass the cell suspension through an 80–100 μm cell strainer and add fresh Locke's solution to produce a final volume of 40–50 mL (Figure 1L).
12. Centrifuge at 48 × *g* for another 3 min; discard the supernatant. Resuspend the pellet by 20 mL culture medium and triturate it with a stripette 5–10 times.
13. Count the cell number in a Neubauer hemocytometer.

   Note: Use low acceleration and deceleration speed when centrifuging to avoid cell damage.

   Note: Avoid air bubbles when triturating or transferring cells to avoid cell damage.

   Note: A typical yield is around 3–9 × 10^7 chromaffin cells from three adrenal glands.

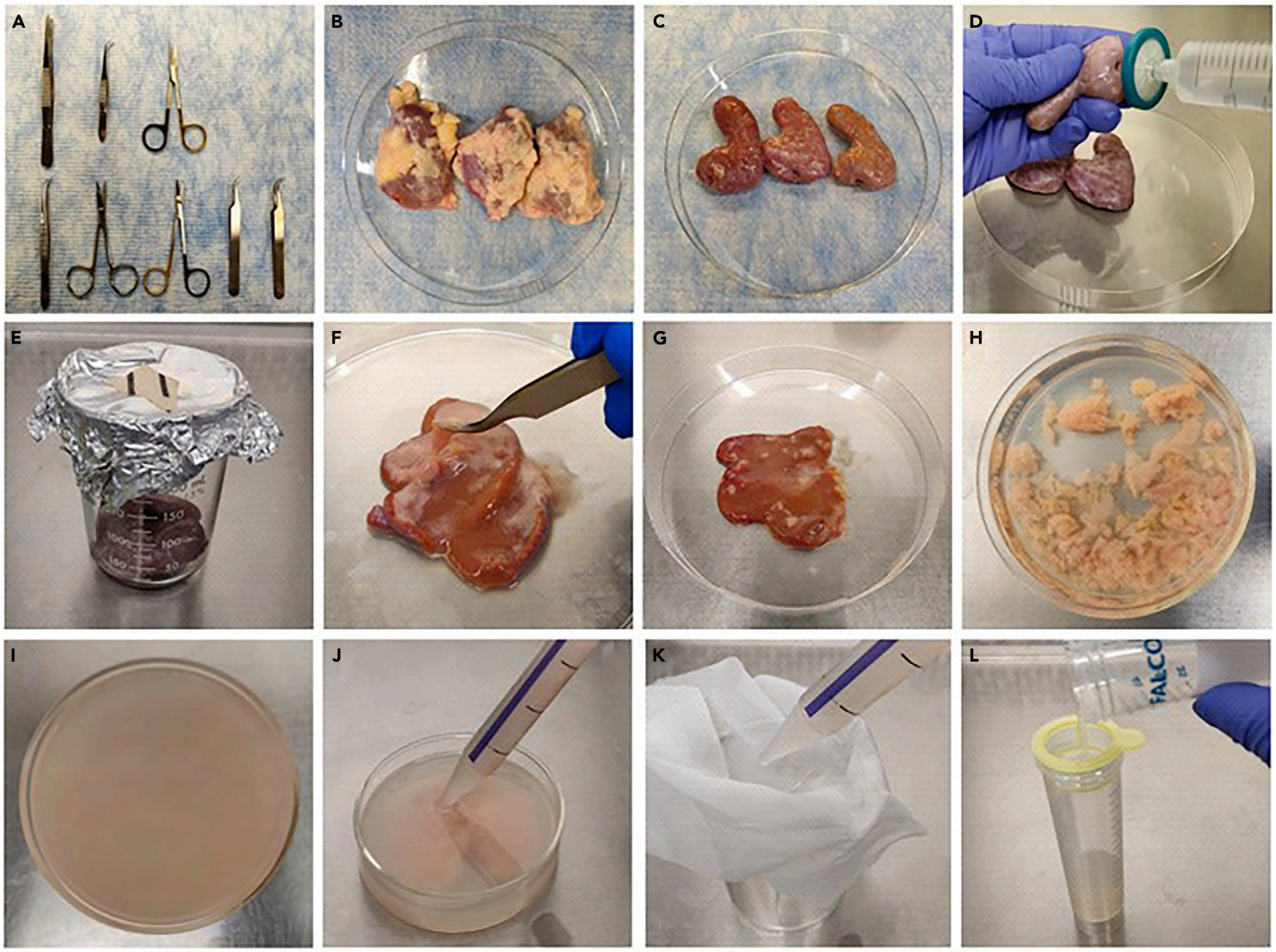

Figure 1. Prepare primary culture of bovine chromaffin cells

(A) Composition of sterile surgical packs (Pack I: upper part; Pack II: lower part).
(B) Bovine adrenal glands from local abattoir.
(C) Bovine adrenal glands after surrounding fat and connective tissue are removed.
(D) Cleaning the adrenal glands with Locke's solution.
(E) Bovine adrenal glands in a beaker, ready for digestion.
(F) Opening bovine adrenal glands and collecting the medulla.
(G) Bovine adrenal glands after collecting the medulla.
(H) Collected medulla in Locke's solution.
(I) Minced medulla in Locke's solution.
(J) Dissociating minced medulla by titrating the material with a 50-mL stripette.
(K) Pass the tissue through an 80–100 μm nylon mesh to remove bulk debris.
(L) Pass the cells through an 80–100 μm cell strainer to further remove debris.

Note: Normally, two repetitions with 10 min each are optimal for digestion. However, the total digestion time may need to be adjusted according to the activity of the collagenase P, which may vary from one batch to another. A total of 18–25 min digestion time is recommended.

Note: In general, optimal exocytosis and endocytosis are usually observed up to 3 days after plating.

Bovine chromaffin cells electroporation – day 1

Timing: 1.5–2 h

Cells are transfected by electroporation using the Basic Primary Neurons Nucleofector Kit and Nucleofector™ 2b device (both Lonza), according to the manufacturer's protocol (https://bioscience.lonza.com/protocol). Here we describe the transfection of mNeonGreen (mNG)-tagged phospholipase C δ1 PH domain (PH-mNG) (Zhao et al., 2016). PH-mNG binds specifically to phosphatidylinositol-4,5-bisphosphate (PtdIns(4,5)P_2, PI(4,5)P_2), a phospholipid that labels the plasma membrane. Other plasmids or siRNAs can be transfected using the same method.

14. Centrifuge 2.5–3 × 10^6 cells at 48 × *g* for 2 min at 20°C–22°C in a 15-mL conical tube.
15. Discard the supernatant and resuspend the cell pellet carefully in 100 μL Nucleofector® solution per sample.
16. Combine 100 μL cell suspension with 1–5 μg PH-mNG plasmid, appropriate amount of siRNA or other substrates.
17. Transfer cell/plasmid suspension into a certified cuvette (sample must cover the bottom of the cuvette without air bubbles).
18. Select program O-005 from the program list of the electroporation device.

Note: Different programs were tested for bovine chromaffin cell electroporation. With program O-005, about 20%–30% transfection efficiency of PH-mNG could be obtained with high viability of cells, whereas other programs tested for bovine chromaffin cells are either with lower efficiency or higher toxicity.

19. Insert the cuvette with the cell/plasmid suspension into the Nucleofector® cuvette holder and start the selected program.
20. Take the cuvette out of the holder once the program is complete.
21. Immediately add 1,500–1,600 μL pre-warmed culture medium to the cuvette and gently aspirate 2–3 times. Transfer 200–300 μL cell suspension onto the 25-mm diameter poly-D-lysine- and laminin-coated coverslips prepared in the culture dish. Use the supplied pipettes and avoid air bubbles in the cell suspension.
22. Incubate cells in a humidified 37°C/9% CO_2 incubator for 1–1.5 h.
23. Add 2 mL pre-warmed culture medium to each dish and incubate cells in a humidified 37°C/9% CO_2 incubator.

Note: Use the slowest speed of the electronic pipette controller when adding culture medium and avoid adding medium directly on cells.

Whole-cell voltage-clamp and capacitance recordings – days 2–4

Timing: 1–5 h

Note: Prepare patch-clamp recording pipettes that have electrode resistances ranging from 2–4 MΩ after filling the pipette with recording electrode internal solution.

In this section, we describe whole-cell voltage-clamp and capacitance recordings, which are performed at room temperature (20°C–22°C) with an EPC-10 amplifier together with the software lock-in amplifier (PULSE, HEKA) (Chiang et al., 2014). A duration of 1 s depolarization is used for stimulation in chromaffin cells. Although this section does not cover imaging, patch-clamp recordings are performed simultaneously with either confocal or STED imaging described in the following two sections. Hence, start the steps described in this section only after the imaging configurations are ready and a good cell has been chosen for either confocal or STED imaging.

Note: The experiments could also be performed at physiological temperature (37°C) using a temperature-controlled recording chamber.

24. Filter recording electrode internal solution using a 1-mL syringe attached with a 0.20-μm Millex-FG syringe filter unit; keep the internal solution on ice during the experiment.
25. Place the coverslip with cells in the chamber (Figures 2A–2E, Methods video S1). Add bath solution with 30–50 μM Atto 655 (A655) or Atto 532 (A532) dye (Figures 2F and 2G, Methods video S1).
26. Choose a healthy transfected chromaffin cell (Figure 3A, Methods video S2), which has a smooth membrane and large cell foot (Figure 3B) visible through the differential interference contrast microscope. Then, move the target cell foot area into the middle of the imaging area.
27. Fill a pipette with recording electrode internal solution. Tap the pipette a few times to eliminate any air bubbles in the tip of the pipette (Methods video S3).
28. Place the glass pipette in the pipette holder (Methods video S3). Apply light positive pressure through a syringe and hold the pressure in the pipette by closing the valve (Methods video S4).
29. Place the pipette tip in the bath with a micromanipulator (Figures 2H–2J, Methods video S4). Set the amplifier to voltage-clamp and correct the pipette offset.
30. Approach the coverslip by moving the micromanipulator and monitoring the pipette height closely. Stop moving the glass pipette just before touching the cell layer on the coverslip and change the settings of the micromanipulator to smooth and slow motion (Methods video S4).
31. Approach the cell body by moving the glass pipette carefully until the tip touches the cell, and a very small dimple is seen on the cell membrane (Methods video S4).
32. Release the positive pressure and apply negative pressure gently with the syringe to obtain a giga Ω seal. Then, adjust the holding potential to -80 mV and press C-fast/Auto to compensate fast capacitance (Methods video S4).
33. To break through the membrane, apply a short suction pulse using the syringe. Press C-slow/Auto to compensate slow capacitance (Methods video S4).
34. For capacitance measurements, the frequency of the sinusoidal stimulus is 1,000–1,500 Hz with a peak-to-peak voltage $\leq$ 50 mV.
35. For stimulation, we used a 1-s depolarization from the holding potential of -80 mV to +10 mV ($depol_{1s}$). We used this stimulus because it induces robust exo-endocytosis as reflected in capacitance recordings (Shin et al., 2018, 2021; Zhao et al., 2016).

Confocal imaging – days 2–4

Timing: 1–5 h

In this section, we describe a typical process for acquiring confocal imaging using a Leica TCS SP5 microscope equipped with a 100 × 1.4 NA oil immersion objective and operated with LAS-X imaging software. The protocol described here is for imaging PH-mNG (excitable at 514 nm, labels plasma membrane), A655 (excitable at 633 nm, labels opened Ω-shaped profiles) and FFN511 (excitable at 458 nm, fluorescent false neurotransmitter for labeling intracellular vesicles). However, this protocol is also applicable to any other fluorescent molecules excitable at other wavelengths (e.g., mTFP-1, Alexa Fluor 488, FFN206). The imaging Z-axis location is fixed to focus on the cell foot, about 200–300 nm above the cell bottom adhering to the coverslip. PH-mNG expression shows the contour of plasma membrane at the XY-plane except the cell foot. At the cell foot, A655 spots can also be observed, reflecting Λ-shape or Ω-shape membrane invaginations (Figure 3B).

36. Incubate cells with 5–10 μM FFN511 for 20–30 min at 37°C to label intracellular vesicles.
37. Set up microscope and imaging chamber (Methods videos S1 and S5).
    a. Turn on Leica SP5 microscope.
    b. Turn on light source.
    c. Select 100 × 1.4 NA oil objective on the microscope.
    d. Prepare 300–600 μL bath solution with 50 μM A655.
    e. Gently remove the FFN511 solution and rinse the chromaffin cells two times with bath solution at 20°C–22°C.

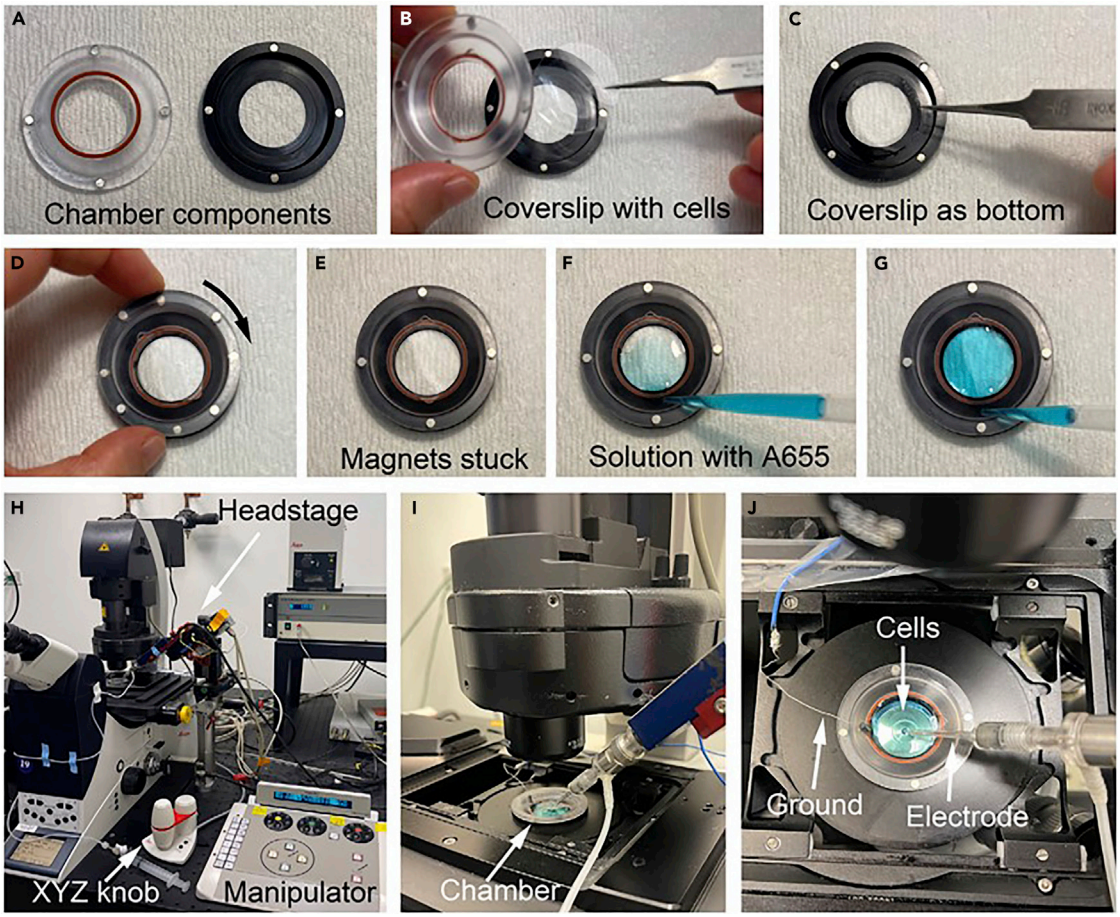

Figure 2. Mount the magnetic chamber with chromaffin cells on the confocal microscope

(A) The magnetic chamber has two components, the upper one (A, left) and the lower one (A, right).

(B and C) Take out of one coverslip with chromaffin cells (B) and put it in the lower component (C).

(D and E) Add the upper component on top of the coverslip with magnets unmatched (D), then rotate it to stick all magnets of the two components (E).

(F and G) Add bath solution with A655 with a pipette.

(H) Mount the chamber on the confocal microscope. The confocal mounting stage is controlled by XYZ adjustment knobs while the electrode of patch-clamp recording is controlled by a micromanipulator via the headstage.

(I) Enough space above the chamber allows movement of the electrode.

(J) Put ground wire into bath solution and then use electrodes to perform patch-clamp recordings on chromaffin cells. See also Methods videos S1 and S3.

f. Use a pair of fine forceps to transfer the coverslip into the magnetic imaging chamber and add 300–600 μL bath solution with 50 μM A655 (Figures 2A–2G).

g. Apply Leica immersion oil to the objective and mount the chamber on the confocal microscope (Figures 2H–2J).

38. Configure Leica software (Methods video S5).

a. Open LAS X software (Figure 4A). Activate the resonant scanner to allow for fast laser scanning, then click "OK" to start the software (Figure 4B).

b. In "Configuration" (Figure 4C), choose "Laser" configuration (Figure 4D) to turn on lasers including Argon laser and HeNe 633 laser (Figure 4E).

c. In "Acquire" (Figure 4F), use "Experiments" to manage files, and "Acquisition" to set the scanning parameters in the following steps (Figure 4G).

d. Select "xyt" time series as the acquisition mode.

e. Choose "512 × 512" format.

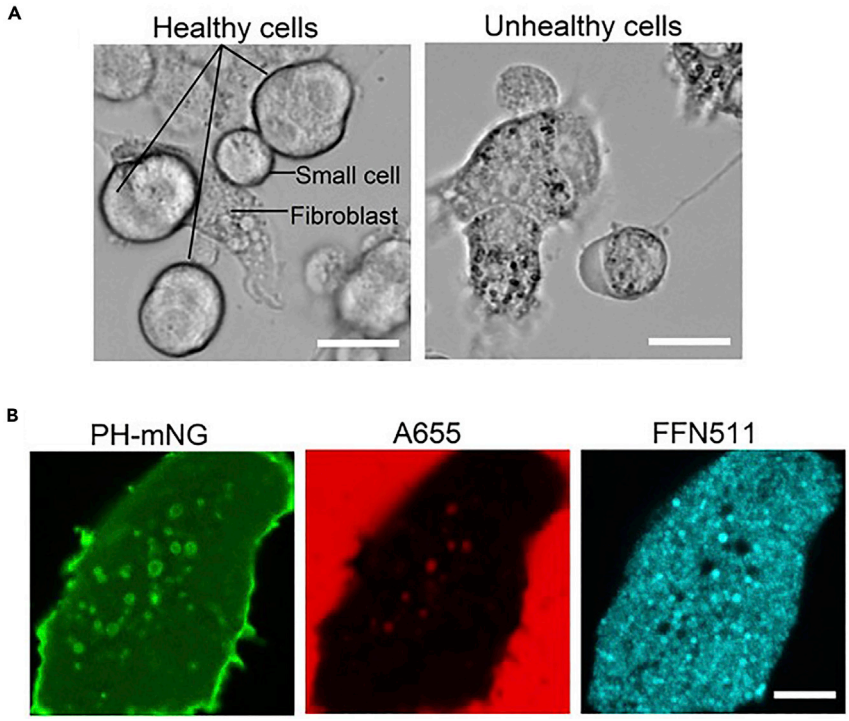

Figure 3. Troubleshooting for healthy cell selection and cell bottom identification in confocal imaging

(A) Healthy cells (left panel) are chosen, and cells too small, fibroblasts, and unhealthy cells (right panel) are avoided for patch-clamp recording and confocal imaging. Scale bars: 20 μm.

(B) Confocal images of PH-mNG (green), A655 (red), and FFN511 (cyan) with XY scanning of the cell foot. Scale bar: 5 μm. See also Methods video S2.

f. Scan speed "8,000 Hz". Make sure to turn on the resonant scanner in step 38a to reach to this scan speed.
g. Choose pinhole 1 A.U.
h. Choose "bidirectional" or "unidirectional" scan mode.
i. Zoom factor: 3–6. The zoom factor will be adjusted according to different cell sizes. The pixel size ranges from about 50 nm to 100 nm.

39. Design appropriate light path configuration to avoid crosstalk between FFN511 and mNG signals. For the fluorophore used in this protocol, low laser power of 514 nm (~1–4 mW) and 458 nm (~2–4 mW) is used to image mNG and FFN511 signal to avoid being bleached, while high laser power (~12–15 mW) of 633 nm is used to bleach A655 dye in closed Ω-profiles or closed vesicles (Methods video S5).
    a. Click "seq" (Figure 4H) to choose sequential scan (Figure 4I) and select "between lines" mode. Click "+" and "-" to add and delete more sequential scans. In sequential "scan 1" (Figure 4I), set excitation and emission laser parameters for FFN511 and A655 (Figures 4J and 4K). In sequential "scan 2" (Figure 4L), set excitation and emission laser parameters for PH-mNG (Figures 4M and 4N).

⚠ CRITICAL: As the spectra of mNG and FFN511 are close to each other, sequential scanning should be chosen to avoid crosstalk between them.

    b. In "scan 1", set the power of 458 nm laser to 10%–20% (~2–4 mW) (Figure 4J), and the collected fluorescence at 465–505 nm with HyD 1 detector (Figure 4K); Set the power of

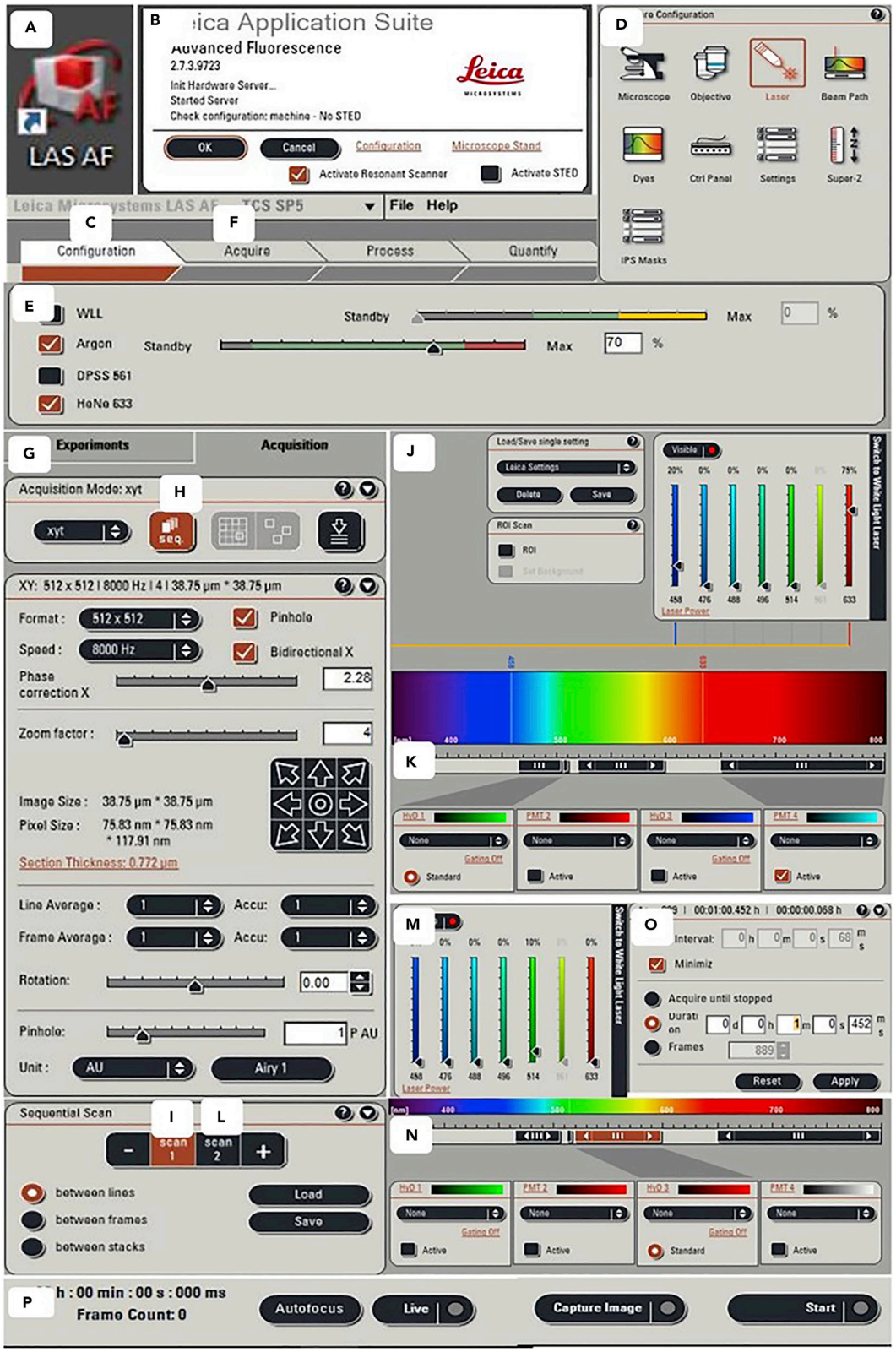
A
LAS AF
B
ica Application Suite
Advanced Fluorescence
2.7.3.9723
Init Hardware Server...
Started Server
Check configuration: machine - No STED
Leica
OK
Cancel
Configuration
Microscope Stand
Activate Resonant Scanner
Activate STED
D
re Configuration
Microscope
Objective
Laser
Beam Path
Dyes
Ctrl Panel
Settings
Super-Z
IPS Masks
File Help
C
F
Configuration
Acquire
Process
Quantify
E
WLL
Standby
Max
0
%
Argon
Standby
Max
70
%
DPSS 561
HeNe 633
G
Experiments
Acquisition
H
Acquisition Mode: xyt
xyt
seq
XY: 512 x 512 | 8000 Hz | 4 | 38.75 µm * 38.75 µm
Format :
512 x 512
Pinhole
Speed :
8000 Hz
Bidirectional X
Phase correction X
2.28
Zoom factor :
4
Image Size :
38.75 µm * 38.75 µm
Pixel Size :
75.83 nm * 75.83 nm
* 117.91 nm
Section Thickness: 0.772 µm
Line Average :
Accu:
Frame Average :
Accu:
Rotation:
0.00
Pinhole:
1
P AU
Unit :
AU
Airy 1
J
Load/Save single setting
Leica Settings
Delete
Save
ROI Scan
ROI
Visible
Switch to White Light Laser
Laser Power
K
HyD 1
PMT 2
HyD 3
PMT 4
None
Gating Off
Standard
Active
M
O
Interval:
Minimiz
Acquire until stopped
Duration
Frames
889
Reset
Apply
I
L
Sequential Scan
scan 1
scan 2
between lines
between frames
between stacks
Load
Save
N
P
h : 00 min : 00 s : 000 ms
Frame Count: 0
Autofocus
Live
Capture Image
Start

Figure 4. Walkthrough of the LAS AF software for configuration to acquire timelapse confocal images

(A) Double click the LAS AF icon to start the software.
(B) Select "Activate Resonant Scanner" and click "OK" to open the software.
(C) In "Configuration", set basic configurations.
(D) In "Experiment Configuration", select different modules. Set "Objective" to 100× oil objective.
(E) Select "Laser" in (D) to turn on Argon laser and HeNe laser. Set the power of Argon laser to 70% of maximum. Maximum power of Argon laser: 25 mW; Maximum power of HeNe laser: 20 mW.
(F) In "Acquire", set basic parameters for confocal scanning.
(G) Choose "Experiments" to create, save, open and rename files, and "Acquisition" to set the scanning parameters. Select "xyt" time series as the acquisition mode; set "Format" to 512 × 512 pixels; set "Speed" to 8,000 Hz; set "Pinhole" to 1 A. U.; check "Bidirectional X"; set "Zoom factor" to 3.0–6.0.
(H) Click "seq" to open "Sequential Scan" module. Select "between lines" in sequential scan module. Click "+" to add sequential scans.
(I) In sequential "scan 1", turn on Argon laser 458 nm and HeNe laser 633 nm to detect FFN511 and A655 signal respectively, detailed parameters shown in (J and K).
(J) Set the power of 458 nm laser to 20%; and the power of 633 nm laser to 75%.
(K) Set the collected fluorescence at 465–505 nm with HyD 1 detector; and the collected fluorescence at 650–800 nm with PMT 4 detector.
(L) In sequential "scan 2", set parameters for 514 nm to detect PH-mNG signal, detailed parameters shown in (M and N).
(M) Set the power of 514 nm laser to 10%.
(N) Set the collected fluorescence at 520–600 nm with HyD 3 detector.
(O) Set 1 min scanning with minimal interval.
(P) When starting to record the patch-clamp data, click "Start" to acquire timelapse confocal images simultaneously. See also Methods videos S4 and S5.

633 nm laser to 60%–75% (~12–15 mW) (Figure 4J), and the collected fluorescence at 650–800 nm with PMT 4 detector (Figure 4K).

c. In "scan 2", set the power of 514 nm laser to 5%–20% (~1–4 mW) (Figure 4M), and the collected fluorescence at 520–600 nm with HyD 3 detector (Figure 4N).

d. Set 1 min scanning with minimal interval, the sampling rate is about 70 ms per frame (Figure 4O).

40. Choose a healthy transfected chromaffin cell (Figure 3A, Methods video S2).

41. Perform patch-clamp recording and start imaging (Figure 4P) when the $depol_{1s}$ protocol starts (Methods video S4).

STED imaging – days 2–4

Timing: 1–5 h

STED images are acquired with a Leica TCS SP8 STED 3× microscope that is equipped with a 100× 1.4 NA HC PL APO CS2 oil immersion objective, white light laser source (WLL) and 592 nm STED depletion laser. The protocol below follows the general guideline for Leica SP8 STED scanning, but details given here are specific to mNG/A532 combination or mNG/FFN511 combination. It is adaptable to other fluorophores with parameter adjustment. The resolution obtained for Leica SP8 STED 3× microscope is ~60 nm for XY and ~150–200 nm for Z (Shin et al., 2018).

⚠ CRITICAL: Use only #1.5 thickness coverslips, which have an ideal thickness of 170 μm for STED imaging. Do not use #1 or other thickness coverslips. The best super-resolution STED images can only be captured with correct (#1.5) thickness glass coverslip, which matches the objectives optimal thickness (0.17 mm). The image intensity and resolution will be reduced significantly even with small deviations from the optimal coverslip thickness.

42. Turn on and warm up the Leica SP8 STED 3× microscope.

a. Turn on the "PC microscope", "Scanner Power", "Laser Power" and "Laser Emission" buttons sequentially to start the machine (Figure 5A).

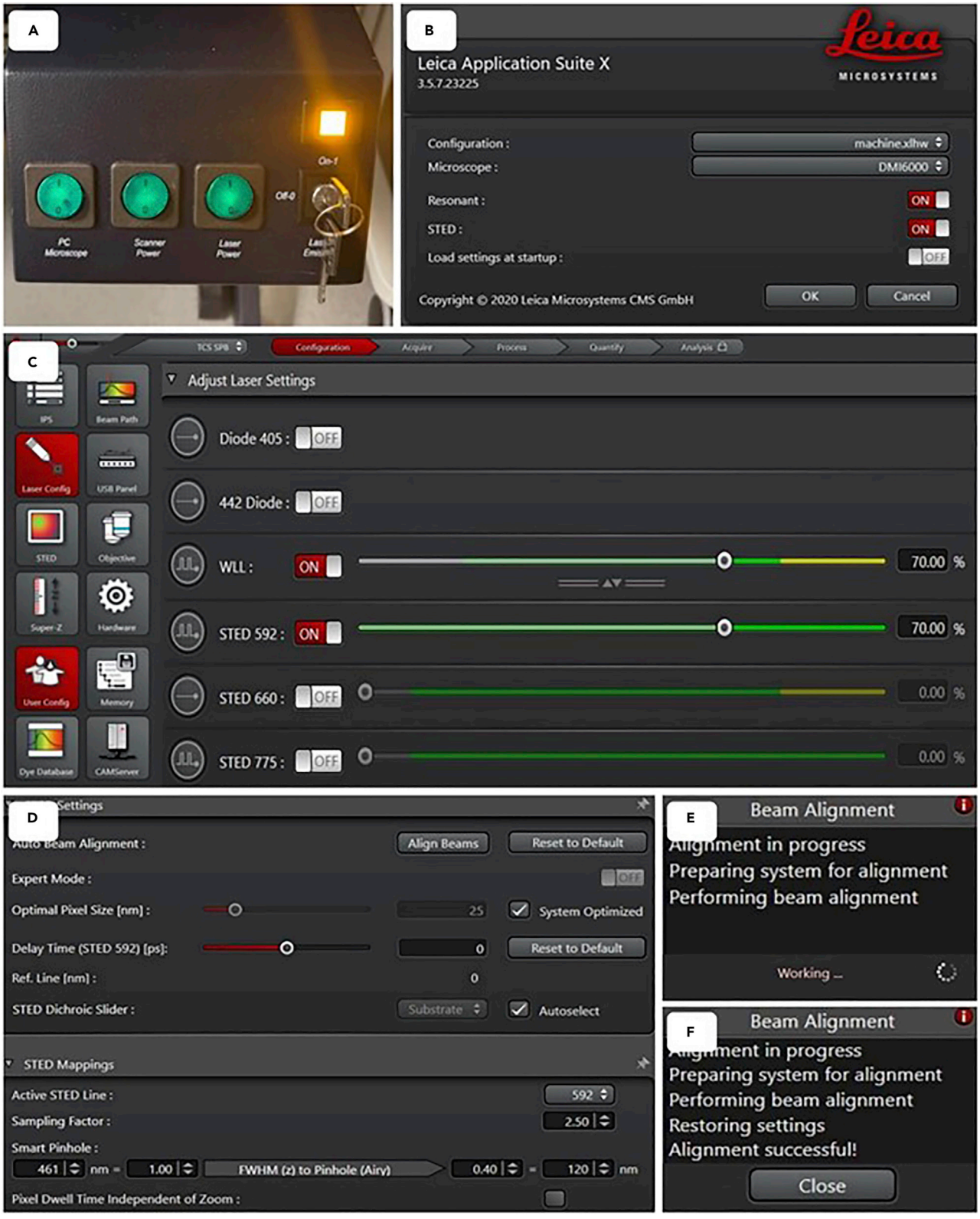
A
PC Microscope
Scanner Power
Laser Power
On-I
Off-0
B
Leica Application Suite X
3.5.7.23225
Leica
MICROSYSTEMS
Configuration :
machine.xlhw
Microscope :
DMI6000
Resonant :
ON
STED :
ON
Load settings at startup :
OFF
Copyright © 2020 Leica Microsystems CMS GmbH
OK
Cancel
C
TCS SP8
Configuration
Acquire
Process
Quantify
Analysis
IPS
Beam Path
Laser Config
USB Panel
STED
Objective
Super-Z
Hardware
User Config
Memory
Dye Database
CAMServer
Adjust Laser Settings
Diode 405 :
OFF
442 Diode :
OFF
WLL :
ON
70.00 %
STED 592 :
ON
70.00 %
STED 660 :
OFF
0.00 %
STED 775 :
OFF
0.00 %
D
Settings
Auto Beam Alignment :
Align Beams
Reset to Default
Expert Mode :
OFF
Optimal Pixel Size [nm] :
25
System Optimized
Delay Time (STED 592) [ps]:
0
Reset to Default
Ref. Line [nm] :
0
STED Dichroic Slider :
Substrate
Autoselect
STED Mappings
Active STED Line :
592
Sampling Factor :
2.50
Smart Pinhole :
461
nm =
1.00
FWHM (z) to Pinhole (Airy)
0.40
=
120
nm
Pixel Dwell Time Independent of Zoom :
E
Beam Alignment
Alignment in progress
Preparing system for alignment
Performing beam alignment
Working ...
F
Beam Alignment
Alignment in progress
Preparing system for alignment
Performing beam alignment
Restoring settings
Alignment successful!
Close

Figure 5. The first step guidance for configuration of Leica SP8 STED 3× microscope

(A) Turn on the "PC Microscope", "Scanner Power", "Laser Power" and "Laser Emission" buttons sequentially from left to right.

(B) Open the LAS X software and turn on the "Resonant" and "STED" to open the resonant scanner and STED laser respectively. Click "OK" to start the LAS X software.

(C) In "Configuration", select "Laser Config" to adjust laser settings. Turn on white light laser (WLL) and set the power to 70% of the maximum. Also turn on the 442 Diode laser if FFN511 is used. Turn on the STED 592 nm depletion laser and set the power to 70% of the maximum. Also turn on other STED lasers such as 660 nm and 775 nm depletion laser if needed. Select "STED" for STED settings, detailed parameters shown in (D).

(D) In "STED Settings", use default values and click "Align Beams" to align STED beams.

(E) Beam Alignment working in progress.

(F) Beam Alignment successful. Click "Close" to finish the STED beam alignment.

b. Open the LAS X software and turn on the "Resonant" and "STED" to open the resonant scanner and STED laser respectively. Click "OK" to start the LAS X software (Figure 5B).
c. Turn on excitation lasers and STED depletion lasers. In "Configuration" of the software, select "Laser Config" to adjust laser settings. Turn on white light laser (WLL) and set the power to 70% of the maximum power (maximum power: 25 mW). Also turn on the 442 Diode laser if FFN511 is used. Turn on the STED 592 nm depletion laser and set the power to 70% of the maximum power (maximum power: 1.5 W). Also turn on other STED lasers such as 660 nm and 775 nm depletion laser if needed (Figure 5C).
d. After warming up the lasers, align STED beams by select "STED" for STED settings (Figure 5C). Check the "Auto Beam Alignment" and "STED Mappings" parameters (Figure 5D), use system optimized and default values and click "Align beams" (Figure 5D). While the beam alignment is working (Figure 5E), lasers through the objective should be seen, do not move any axis of the microscope. Once it is successful, click "Close" to finish the STED beam alignment (Figure 5F).

Note: Before beam alignment, let the lasers warm up for 10–20 min. In STED laser beam alignment step, no cell samples are need.

43. Prepare coverslip and imaging chamber (Figure 2).
    a. Prepare 300–600 μL 30 μM A532 bath solution.
    b. Gently rinse the chromaffin cells two times with bath solution at 20°C–22°C.
    c. Use a pair of fine forceps to transfer the coverslip on the chamber and add 300–600 μL 30 μM A532.
44. Set up scanning parameters. Typical settings:
    a. Scan mode: xyt or xzt, sequential scan and between lines (Figure 6A).
    b. Line scan speed: 8,000 Hz (Figure 6B).
    c. Scan direction: Bidirectional or Unidirectional (Figure 6B).
    d. Zoom: 5.0–6.0 (Figure 6B). The zoom factor could be adjusted according to different cell sizes.
    e. Image resolution: 1248 × 1000 (xyt scanning) and 1248 × 150 (xzt scanning).
    f. Image size: 19.38 μm × 15.52 μm (xyt scanning) and 19.38 μm × 2.32 μm (xzt scanning).
    g. Pixel size: 16–20 nm.
    h. Line Average (scan a line for multiple times before move to the next line, and average the pixel values), Frame Average (scan a frame for multiple times, and average the pixel values), Line Accumulation (scan a line for multiple times and sum the pixel values), and Frame Accumulation (scan a frame for multiple times and sum the pixel values) are all set to 1.

Note: Both Line-based and frame-based scanning modes have same effect, but the execution ways are different. Multi-time scanning with any of the four modes extends the total scanning time. Average reduces noise and improves signal by averaging each point together, whereas accumulation increases signal intensity to improve signal-to-noise ratio

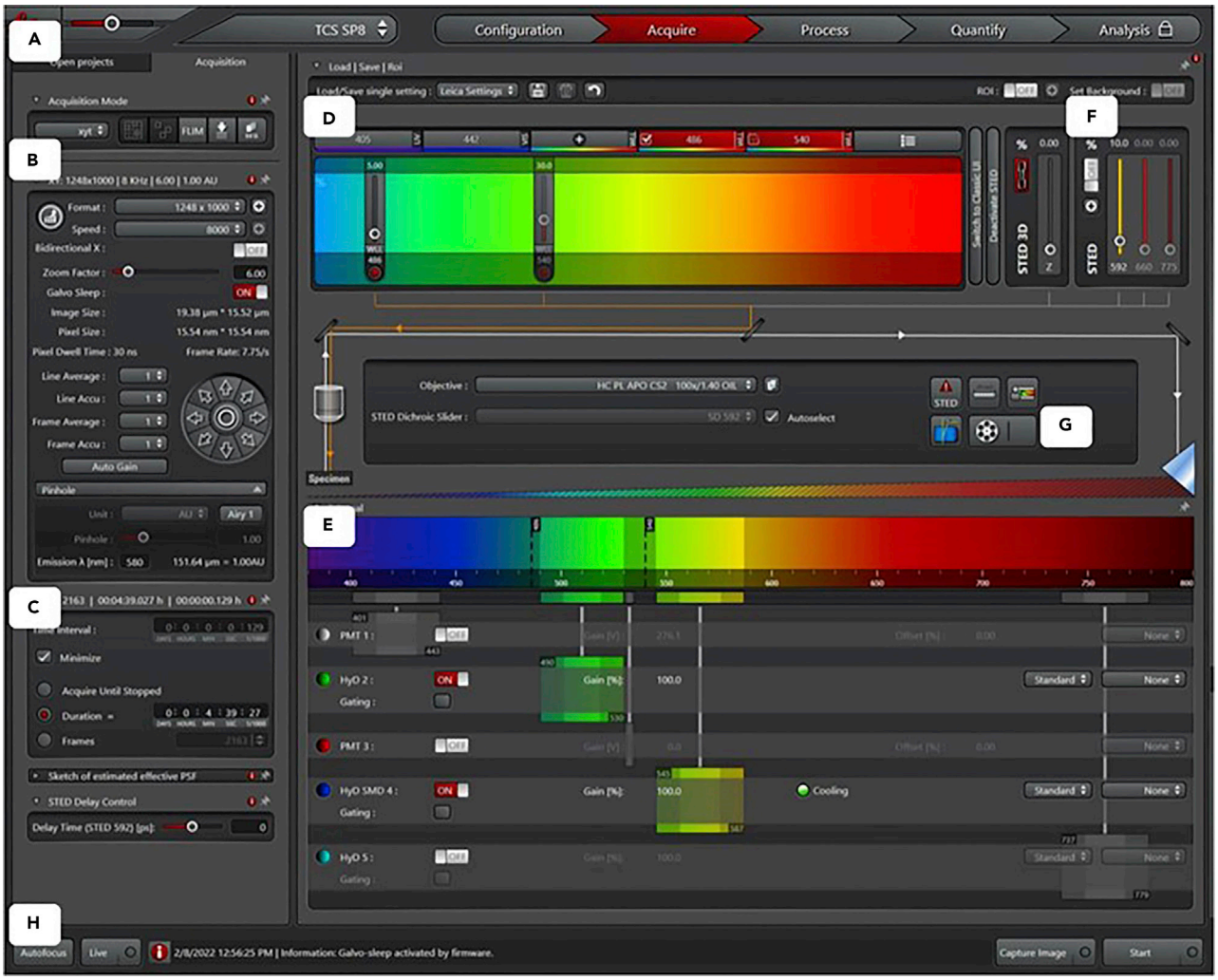

Figure 6. The second step guidance for configuration of Leica SP8 STED 3× microscope

(A) Click "Acquire" of the software, and in "Acquisition", select "xyt" or "xzt" mode, and select "SEQ" for sequential scanning.

(B) Set "Format" to 1248 × 1000 for xyt scanning or 1248 × 150 for xzt scanning; set "Speed" to 8,000 Hz; keep "Bidirectional X" off; set "Zoom factor" to 6; set "Line Average", "Line Accu", "Frame Average", and "Frame Accu" to 1; set "Pinhole" to 0.5 A. U.

(C) Set "Time interval" to "minimize", and "Duration" to 90 s.

(D) Excitation laser selection and power adjustment. For mNG/A532, set 486 nm at 5% and 540 nm at 30%; For mNG/FFN511, set 505 nm at 5% and 442 nm at 30%.

(E) Detector selection and collection range adjustment. For mNG/A532, collect emission at 490–530 nm and 545–587 nm. For mNG/FFN511, collect emission at 510–587 nm and 447–490 nm, with sequential scanning.

(F) STED depletion laser selection and power adjustment. Set 10% for mNG and 5% for A532 or FFN511.

(G) Use the Fluorifier Disc Settings to set the notch filters to NF 445/594.

(H) When start to record the patch-clamp data, click "Start" to acquire timelapse STED images simultaneously.

by adding each point together. By setting the value to 1, we do not use these functions. But these functions can be used to improve signal-to-noise ratio.

i. Pinhole: 0.5 AU (75.8 μm) (Figure 6B), which can be adjusted in a range of 0.4–0.6 AU.
j. Time Interval: minimize (Figure 6C).
k. Gating for HyD detector: 1.0–6.5 ns (Figure 6E).
l. Notch Filter: NF 445/594 (Figure 6G).

45. Establish STED light paths. Typical settings for mNG/A532 combination:
    a. mNG is excited at 486 nm (~1–5 mW) (Figure 6D) and the gain of the high-sensitivity HyD detector (490–530 nm) is 100 (Figure 6E).
    b. A532 is excited at 540 nm (~5 mW) (Figure 6D) and the gain of the high-sensitivity HyD detector (545–587 nm) is 100 (Figure 6E).
    c. 592 nm STED depletion beam is set to 10%–40% (~105–420 mW) and 5% (~52.5 mW) for mNG and A532 respectively (Figure 6F).

    Typical settings for mNG/FFN511 combination:
    d. mNG is excited at 505 nm (~1–5 mW) and the gain of the high-sensitivity HyD detector (510–587 nm) is 100.
    e. FFN511 is excited at 442 nm (~3–5 mW) and the gain of the high-sensitivity HyD detector (447–490 nm) is 100.
    f. 592 nm STED depletion beam is set to 10%–40% (~105–420 mW) and 5% (~52.5 mW) for mNG and FFN511, respectively.
46. Find a healthy transfected chromaffin cell under bright field and epifluorescence (Figure 3).

⚠ CRITICAL: Use a low level of white light and epifluorescence for cell searching because strong light exposure bleaches the fluorescence of interest and causes cell phototoxicity.

47. Perform whole-cell voltage-clamp, capacitance recordings and STED imaging with the target cell:
    a. Find the cell and get a giga Ω seal.
    b. Break the cell and hold it at -80 mV.
    c. Before stimulation, find the cell foot area with xyt confocal scanning (Figure 3B).

Note: Minimize confocal lasers to 1% (~0.175 mW) for either mNG/A532 or mNG/FFN511 to avoid bleaching.

    d. Switch to xzt mode (Figures 6A and 6B), focusing on the plasma membrane.

Note: Minimize confocal lasers to 1% (~0.175 mW) (Figure 6D) for either mNG/A532 or mNG/FFN511 to avoid bleaching.

    e. Turn off the laser, then set back to the appropriate confocal (Figure 6D) and depletion laser power (Figure 6F), which has been depicted in step 45.
    f. Start the $depol_{1s}$ and STED imaging at the same time (Figure 6H). In general, the total recording time is 90 s or longer (Figure 6C).

⚠ CRITICAL: STED laser exposure to cells only after correct imaging configuration and successful patch-clamp operation.

Note: Patch less than 5 cells per coverslip, then change to a fresh coverslip.

STED image deconvolution using Huygens Professional – days 2–4

Timing: 0.5–3 h/image

48. Run Leica LAS X software.
    a. Open a project (experimental data with *.lif file).
    b. Right click the raw data and export it to Huygens Professional.

49. Run Huygens Professional program.
    a. In Huygens Professional (Figure 7A), run "Edit Microscopic Parameter" in "Edit" menu and confirm the parameters, including XYZ pixel sizes, numerical aperture, and pinhole size, of the raw STED image (Figure 7B). All parameters should be consistent with the properties of raw data.
    b. Run "Deconvolution wizard" in "Deconvolution" menu of the software (Figure 7C). Raw images can be deconvoluted by entering this wizard (Figure 7D). Check the parameters of the deconvolution of each channel step-by-step, such as the mapping functions, background estimation, deconvolution algorithm, signal to noise ratio and maximum iterations (Figure 7E). Deconvolution can be done by using the default parameters (Figure 7F). However, different parameters can be adjusted until the deconvolution images (Figure 7G) cannot be improved further. In general, the most important parameter is "Maximum Iterations", and the parameter can be between 10 to 40. More details can be found in the user guide of the software (https://depts.washington.edu/digmicro/huygens_pdf/ProfessionalUserGuide1505.pdf).
50. When deconvolution is over, export the deconvolution file back to LAS X. The deconvolution image can be found in "Imported from Huygens" folder.

Electron microscopy (EM) – days 3–7

Timing: 1 week

In this section, electron microscopy is performed after a 90-s application of 70 mM potassium solution in bovine chromaffin cells. We use high potassium solution to induce depolarization of every cell so that every cell can be examined with electron microscopy. Patch-clamp and depolarization of single cells are not suitable for EM examination, because it is difficult to identify the individual cell being patch-clamped.

51. Take the coverslips and immerse them in a solution containing 70 mM KCl, 60 mM NaCl, 10 mM glucose, 10 mM HEPES, 2 mM $CaCl_2$, and 1 mM $MgCl_2$ (pH 7.3, adjusted with NaOH) for 90 s (Figure 8A).
52. Fix the cultures with 2% glutaraldehyde/2% paraformaldehyde/4% tannic acid/0.1 M sodium cacodylate for 15 min at 20°C–22°C.
53. Switch to 2% paraformaldehyde/2% glutaraldehyde/0.1 M sodium cacodylate fixative solution for 15 min at 20°C–22°C.
54. Wash the preparation with 100 mM glycine in 0.1 M sodium cacodylate buffer for 1 min at 20°C–22°C.
55. Wash 3 × 5 min in 0.1 M sodium cacodylate at 20°C–22°C.

Pause point: The sample can be stored at 4°C for 1–2 weeks.

56. Start mixing Epon resin (Embed-812) and leave it on a rotator for 1–2 h.
57. Treat with 1% osmium tetroxide in 0.1 M sodium cacodylate for 40 min.
58. Rinse in 0.1 M sodium cacodylate to wash osmium tetroxide.
59. Rinse in double-distilled water (DDW).
60. Dehydrate in ethanol as follows:
    a. 50% Ethanol (EtOH) 1 × 5 min.
    b. 70% EtOH 2 × 5 min.
    c. 2% uranyl acetate in 70% EtOH 30 min (prepare 1:1 Epon/EtOH mix).
    d. 70% EtOH 2 × 10 min.
    e. 85% EtOH 2 × 5 min.
    f. 95% EtOH 2 × 5 min.
    g. 100% EtOH 2 × 5 min.

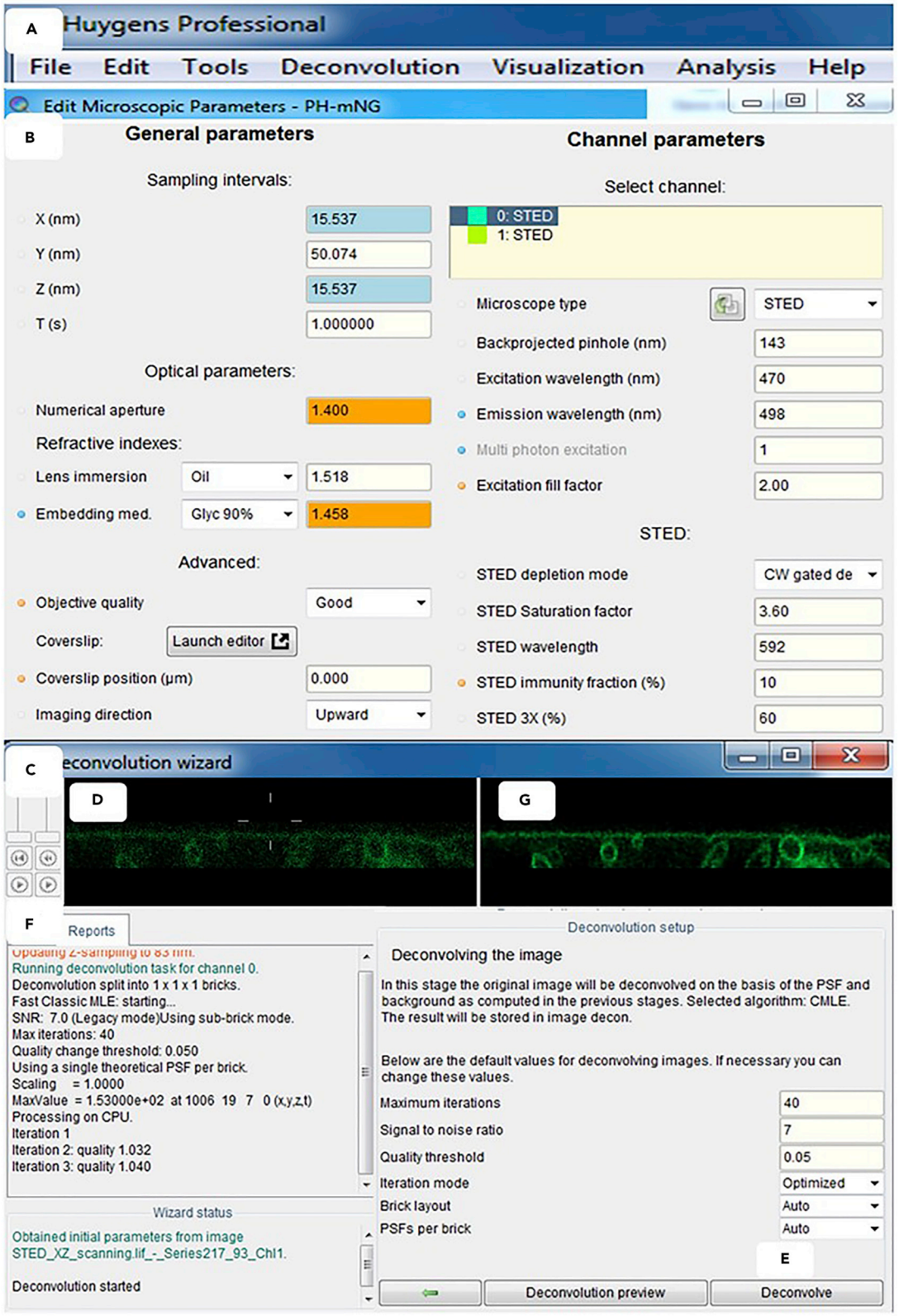
A
Huygens Professional
File Edit Tools Deconvolution Visualization Analysis Help
Edit Microscopic Parameters - PH-mNG
B
General parameters
Sampling intervals:
X (nm) 15.537
Y (nm) 50.074
Z (nm) 15.537
T (s) 1.000000
Optical parameters:
Numerical aperture 1.400
Refractive indexes:
Lens immersion Oil 1.518
Embedding med. Glyc 90% 1.458
Advanced:
Objective quality Good
Coverslip: Launch editor
Coverslip position (µm) 0.000
Imaging direction Upward
Channel parameters
Select channel:
0: STED
1: STED
Microscope type STED
Backprojected pinhole (nm) 143
Excitation wavelength (nm) 470
Emission wavelength (nm) 498
Multi photon excitation 1
Excitation fill factor 2.00
STED:
STED depletion mode CW gated de
STED Saturation factor 3.60
STED wavelength 592
STED immunity fraction (%) 10
STED 3X (%) 60
C
econvolution wizard
D
G
F
Reports
Running deconvolution task for channel 0.
Deconvolution split into 1 x 1 x 1 bricks.
Fast Classic MLE: starting...
SNR: 7.0 (Legacy mode)Using sub-brick mode.
Max iterations: 40
Quality change threshold: 0.050
Using a single theoretical PSF per brick.
Scaling = 1.0000
MaxValue = 1.53000e+02 at 1006 19 7 0 (x,y,z,t)
Processing on CPU.
Iteration 1
Iteration 2: quality 1.032
Iteration 3: quality 1.040
Wizard status
Obtained initial parameters from image
STED_XZ_scanning.lif_-_Series217_93_Ch1.
Deconvolution started
Deconvolution setup
Deconvolving the image
In this stage the original image will be deconvolved on the basis of the PSF and background as computed in the previous stages. Selected algorithm: CMLE. The result will be stored in image decon.
Below are the default values for deconvolving images. If necessary you can change these values.
Maximum iterations 40
Signal to noise ratio 7
Quality threshold 0.05
Iteration mode Optimized
Brick layout Auto
PSFs per brick Auto
E
Deconvolution preview
Deconvolve

Figure 7. Parameters setting and guidance for deconvolution

(A and B) After exporting .lif data file into Huygens Professional software, select "Edit" menu (A) to choose "Edit Microscopic Parameters" (B). Make sure the "General parameters" (B, left) such as sampling intervals and optical parameters are consistent with the raw data collected with STED microscope. In "Channel parameters" (B, right), select "STED" for microscope type, review and set all parameters verified.

(C) Select "Deconvolution" menu (A) to choose "Deconvolution wizard" (C).

(D) The raw data will present in the "Deconvolution wizard" window.

(E) Enter the step-by-step deconvolution process, including PSF selection, cropping, inspecting the image histogram, background estimation, deconvolution setup, and then click "Deconvolve" to run the deconvolution.

(F) Maximum iterations, signal to noise ratio, quality threshold, and integration mode could be automatic or adjusted by users. Reports will be shown after deconvolution finished, and the iteration numbers will be optimized by the software.

(G) The deconvoluted image will be shown for users to review. Save the deconvoluted images for analysis.

⚠ CRITICAL: Slide should not dry even for a moment during these steps. Always leave some solution on the top when they are switched.

61. Put into a foil dish filled with 1:1 Epon/EtOH mix.
62. Replace Epon/EtOH mix with Epon resin alone for 2 h, switch resin and leave for additional 2 h.
63. Fill molds to brim. Wipe the backs of coverslips with filter paper, and invert over filled circular molds.

Note: Make sure there are no air bubbles under the coverslip.

64. Polymerize Epon at 50°C for 14–18 h.
65. Transfer to 60°C oven for several days to harden (at least 36 h).

Pause point: The sample can be stored at 20°C–22°C in a desiccator dry box for 2 years.

66. Immerse and hold the block in liquid nitrogen for 30 s. Apply gentle pressure on the edge of the coverslip to remove it. Ensure that no glass is left on the surface.
67. Trim the block and cut cross sections of 70 nm using a Leica UC7 Ultramicrotome (Figure 8B) and place them on a 200 mesh pioloform coated index grid.
68. Counterstain sections with uranyl acetate for 5 min and 3 min with lead citrate. Each counterstain is followed by serial washes using DDW.

Pause point: The sample can be stored at 20°C–22°C in a desiccator dry box for several months.

69. Single images were collected at up to 73,000 × magnification on a JEOL JEM-200CX, 120 kV electron microscope with an AMT XR-100 CCD.

EXPECTED OUTCOMES

Applying this protocol to chromaffin cells, we overexpressed PH–mNG to label the plasma membrane, add cell-impermeable dye A655 or A532 in the bath solution to label the fusion-generated Ω-profile, and load vesicles with fluorescent false neurotransmitter FFN511 to detect vesicle fusion and content release. Chromaffin cells were stimulated with depol1s to induce exocytosis and endocytosis. Confocal and STED imaging were performed to observe fusion pore dynamics, transmitter release (Figures 9 and 10) and endocytic membrane dynamics (Figure 11). Three modes of fusion pore dynamics were observed: 1) close-fusion (also called kiss-and-run), involving fusion pore opening and closure, 2) stay-fusion, involving fusion pore opening and maintenance of the open pore for a long time, and 3) shrink-fusion, involving shrinkage of the Ω-shape membrane profile generated by fusion until the vesicle merges completely with the plasma membrane (Chiang et al., 2014; Shin et al., 2018, 2020; Wen et al., 2016; Zhao et al., 2016). Various endocytic modes such as slow, fast, and ultrafast endocytosis have been found to be mediated primarily by two forms of pore

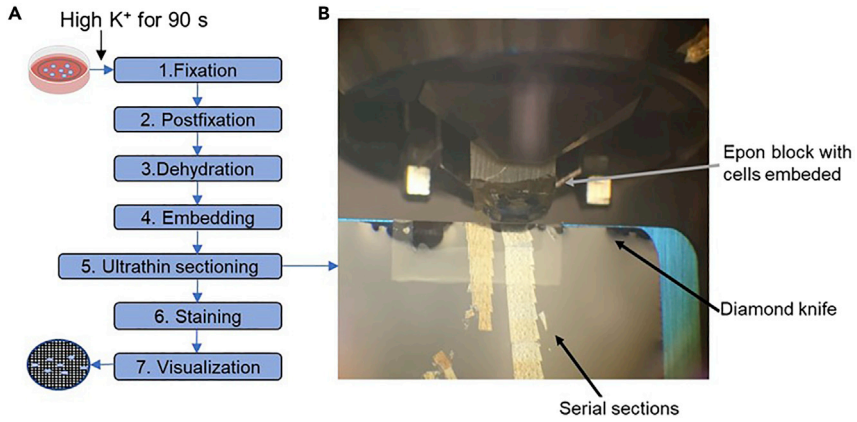

Figure 8. Electron microscopy procedures

(A) Chromaffin cells were stimulated with 70 mM K^+ for 90 s and several steps were applied for visualization of Ω-profile structures.

(B) A ultramicrotome (Leica UC7) used for sectioning cells.

closure, fusion pore closure (e.g., Figure 9A) and pore closure of Ω-profiles preformed before application of a depolarizing stimulus (Figure 9D) (Shin et al., 2021).

Cells were also exposed to high potassium to induce depolarization, and EM imaging was used to observe plasma membrane or vesicle structure (Figure 12). Representative confocal, super-resolution STED and EM imaging are shown in Figures 9, 10, 11, and 12.

Confocal imaging resolves three fusion modes: Close-, stay-, and shrink-fusion

Confocal imaging of PH–mNG, A655 and FFN511 was performed at the XY plane with a fixed Z plane about 100–200 nm above the cell bottom membrane (XY/Z_{fix} imaging, Figures 3B and 9). PH–mNG and FFN511 were excited with ~1–4 mW and ~2–4 mW laser power respectively, while A655 was excited with ~12–15 mW laser power.

Vesicle fusion was detected as a FFN511 spot fluorescence (F_{FFN}) decrease with concurrent PH–mNG fluorescence (F_{PH}) and A655 spot fluorescence (F_{655}) increases due to FFN511 release and PH–mNG/A655 spot formation via diffusion from the plasma membrane/bath into fusion-generated Ω-profiles (Figures 9A–9C) (Shin et al., 2018, 2021). Three modes of fusion pore dynamics were observed: (1) close-fusion (also called kiss-and-run), detected as F_{655} dimming, due to pore closure that prevents bleached A655 (by strong excitation) from being exchanged with fluorescent A655 in the bath, while F_{PH} sustains or decays with a delay due to conversion of $PI(4,5)P_2$ into PI(4)P and/or vesicle fission after closure (Figure 9A), (2) stay-fusion, detected as persistent PH–mNG/A655 spot presence (Figure 9B), and (3) shrink-fusion, detected as the approximately parallel decrease of spot-size, F_{655} and F_{PH} due to shrinkage of the fusing Ω-profile (Figure 9C) (Shin et al., 2018, 2020, 2021).

Spots preformed before depol1s were observed. These spots were identified as PH-mNG spots (or rings) overlapped with A655, but not FFN511 spots. They reflect mostly preformed Ω-profiles (pre-Ω) (Shin et al., 2021). Depol1s induced closure of these preformed Ω-profiles, detected as F_{655} dimming while F_{PH} sustained or dimmed with a delay (Figure 9D). These preformed spot closures constitute a major endocytic mechanism underlying many forms of endocytosis, including rapid and slow endocytosis (Shin et al., 2021).

STED imaging visualizes fusion pore opening, constriction, closure, and content release

For STED imaging, A532 was used instead of A655 to label fusion-generated Ω profiles. PH–mNG and FFN511 or PH–mNG and A532 were imaged at the XZ plane with a fixed Y plane every 26–

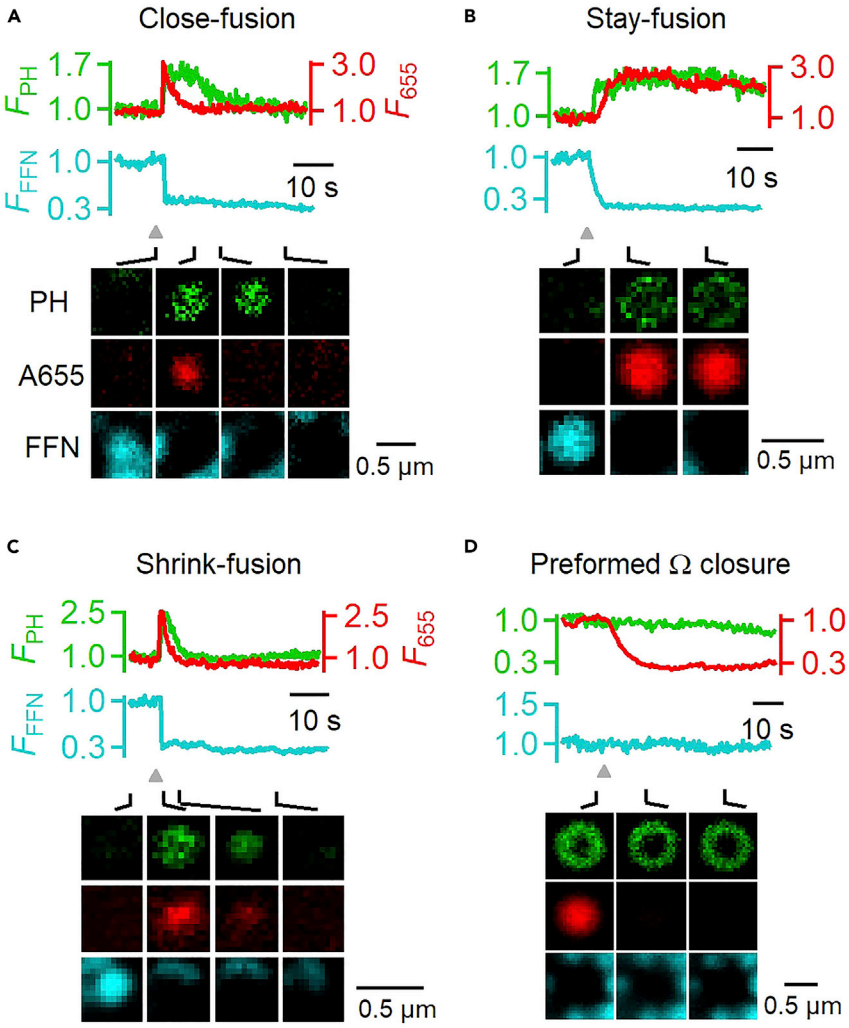

Figure 9. Vesicle fusion and preformed Ω closure observed by confocal imaging

(A–C) Depol$_{1s}$ was used to induce exocytosis and endocytosis and confocal XY/Z$_{fix}$ imaging was performed at the cell bottom. PH, A655 and FFN511 fluorescence (F_{PH}, F_{655} and F_{FFN}) were normalized to baseline. Sample confocal XY/Z$_{fix}$ images (at times indicated with lines) were shown. Three modes of vesicle fusion were identified: close-fusion (A), stay-fusion (B) and shrink-fusion (C).

(D) The identification of fusion modes is described in the main text. Preformed Ω profile closure (D) was also observed. Gray triangle, depol$_{1s}$. Scale bar: 0.5 μm for both X and Y axis.

Figure reprinted with permission from Shin et al. (2021).

200 ms (XZ/Y$_{fix}$ scanning). PH–mNG and FFN511 were excited with ~1–5 mW and ~3–5 mW laser power respectively, while A532 was excited with ~5 mW laser power. For A532 of STED imaging, ~5 mW is sufficient because 592 nm depletion laser also contribute to A532 dye bleaching.

Depol1s induced vesicle fusion at the plasma membrane, allowing for PH-mNG diffusion from the plasma membrane into the fusion-generated Ω-profile to label the Ω-profile and release of FFN511 through the pore of the Ω-profile (Figure 10A) (Shin et al., 2018). Figure 10A shows an example of a PH-mNG-labeled Ω-profile with a visible fusion pore that releases FFN511. Fusion pore opening, detected as the sudden appearance of a PH-mNG labeled Ω-shape profile with a visible pore, may constrict and become invisible within two image frames (92 ms in Figure 10B). Fusion pore constriction may be followed by pore closure, detected as A532 fluorescence (F_{532}) dimming while F_{PH} sustains or decays after a delay (Figure 10B), because pore closure prevents

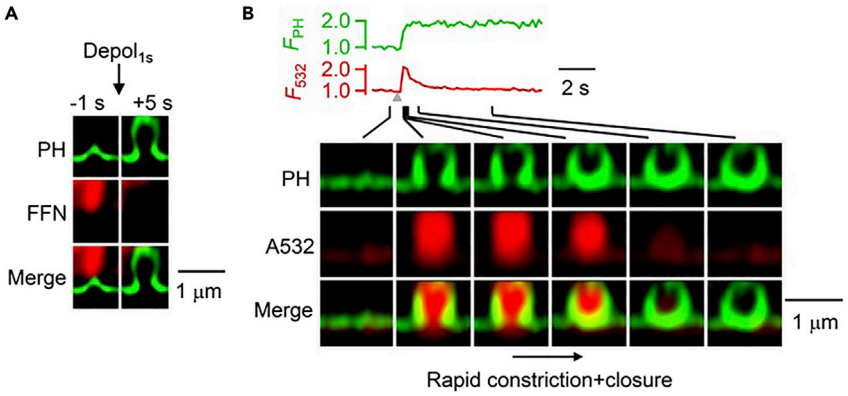

Figure 10. Vesicle fusion, neurotransmitter release, and fusion pore closure observed by STED imaging

(A) Depol$_{1s}$ induced vesicle fusion at the plasma membrane. PH/FFN STED images before (-1 s) and after (+5 s) depol1s are shown. After depol$_{1s}$, fusion pore and FFN511 release can be observed.

(B) PH/A532 STED imaging was performed with XZ/Y$_{fix}$ scanning. F_{PH}, F_{532} (normalized to baseline), and sampled images at the times indicated with lines showing fusion pore dynamics. At the first frame fusion pore was observed, it reached the maximal size, which indicates rapid opening. Fusion pore constricted rapidly and became invisible in two image frames (96 ms) and closed (impermeable to A532). Gray triangle, depol$_{1s}$.

Figure reprinted with permission from Shin et al. (2018).

bleached A532 (by strong excitation) from exchanging with fluorescent A532 in the bath (Shin et al., 2018).

STED imaging observing endocytic transitions mediated by membrane invagination, Λ base constriction, and Ω pore constriction

STED XZ/Y$_{fix}$ scanning of PH-mNG and A532 can also be used to visualize depol1s-induced endocytic membrane dynamics. We observed the transition from flat membrane (Flat) to oval/round-shaped vesicles (O) via the intermediate Λ-shape and Ω-shape structures (Flat→Λ→Ω→O, Figure 11). Ω→O transition (Ω pore closure) was detected as F_{532} (excited strongly) dimming, while F_{PH} (excited weakly) sustains (Figure 11) because pore closure prevents bleached A532 (by strong excitation) from exchanging with fluorescent A532 in the bath, resulting in F_{532} decay (Shin et al., 2018).

EM imaging of Ω-profiles

To examine Ω-profiles with different pore sizes with EM, bovine adrenal chromaffin cells were stimulated for 90 s using a solution containing 70 mM KCl. Ω-profiles with pore diameters of 12–430 nm during KCl-induced depolarization (92 ± 12 nm, 53 pores) were observed (Figures 12A and 12B), similar to the STED-measured visible pore range (Shin et al., 2018). The diameter for pores > 60 nm (152 ± 18 nm, 25 pores, Figures 12A and 12B) was similar to the STED-measured pore size at ~60 nm resolution (Shin et al., 2018).

LIMITATIONS

The protocol requires fluorescent labeling of the cell membrane. Super-resolution STED microscopy requires a high-power depletion laser, which may cause photobleaching and phototoxicity to cells. To avoid this problem, we usually limit the duration of STED imaging to less than 90 s.

In this protocol, 1-s depolarization was used for confocal and STED imaging, whereas 90-s high potassium application was used for electron microscopy. It is possible to distinguish between exo- and endocytosis with live-cell confocal and STED imaging, but is difficult with EM.

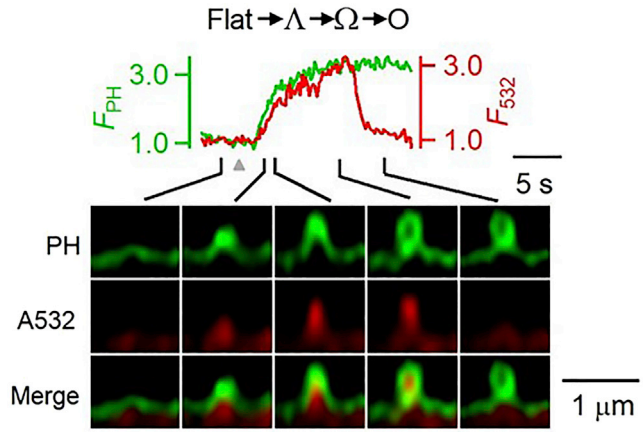

Figure 11. STED microscopy visualizes Flat→Λ→Ω→O endocytic transitions

F_{PH} and F_{532} (normalized to baseline) and STED XZ/Y_{fix} images (at times indicated with lines) for a Flat→Λ→Ω→O transition were shown. Gray triangle, $depol_{1s}$; Ω→O detection is described in the main text.

Figure reprinted with permission from Shin et al. (2021).

We used 1-s depolarization to induce robust exo- and endocytosis, which significantly increases our chance of capturing individual exo- and endocytic events at the cell plasma membrane. Furthermore, the exo- and endocytic events were observed mostly within 20 s after the depolarization, which avoids long-term exposure to high-power laser lights needed for STED microscopy. However, 1-s depolarization is not a physiological stimulation. We expect that the exo- and endocytic events induced by trains of action potentials are similar to those induced by 1-s depolarization, although the ratio of different modes of exo- and endocytosis might be somewhat different.

The use of photobleaching of an external dye such as A655 and A532 in this protocol allows us to determine the timing of membrane fission. The temporal precision is determined mostly by the time constant of bleaching and the signal-to-noise ratio of the fluorescent dye in the vesicles. The bleaching time constant is about 2–3 s with the use of high laser power (~12–15 mW) for dye bleaching. With the bleaching kinetics fitted, we regard the starting point for the dye fluorescent intensity to drop below the noise level as the fission time. The temporal precision is ~0.1–0.2 s. However, it can be further improved by increasing the laser power and improving the signal-to-noise ratio if necessary.

As the local abattoir provides mainly male animals, the majority of adrenal glands in the study are from males, which limits the study of gender differences.

TROUBLESHOOTING

Problem 1

Low transfection efficiency (in bovine chromaffin cells electroporation – day 1 section, step 18).

Potential solution

The normal transfection efficiency in chromaffin cells is around 20%–30%. However, it could be somehow less than 10%. In most cases, this low transfection efficiency is caused by under-digestion of chromaffin tissue. This problem can be overcome by increasing 5–10 min more to the enzyme treatment time during primary culture.

Problem 2

Hard to succeed for patch-clamp (in whole-cell voltage-clamp and capacitance recordings – day 2–4 section, step 32).

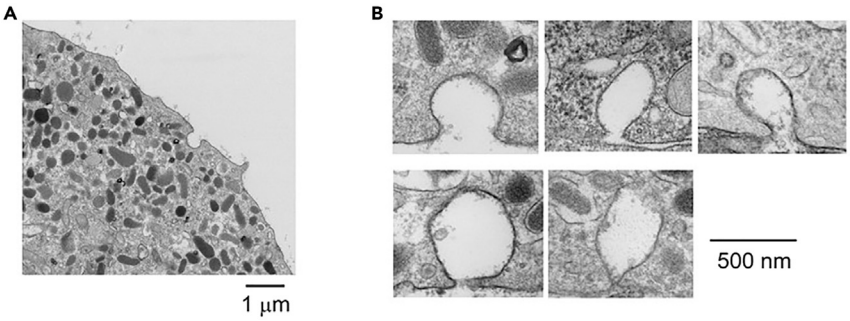

Figure 12. Sample EM images showing Ω-profiles with different pore sizes
(A) EM image of a cell.
(B) sample EM images of Ω-profiles with different pore sizes. Cells were in 70 mM KCl for 90 s.
Figure reprinted with permission from Shin et al. (2018).

Potential solution

Choose healthy cells and avoid unhealthy cells (Figure 3A, Methods video S2). Make sure the pipette tip has the correct size and resistance (Methods video S4).

Problem 3

FFN511 and/or mNG signal is easy to be bleached (in confocal imaging – day 2–4 section, step 39).

Potential solution

Test a lower laser power as a starting point. Minimize the exposure to laser before imaging.

Problem 4

Less than 5 fusion events per cell after stimulation in XY/Z_{fix} imaging (in confocal imaging – day 2–4 section, step 41).

Potential solution

Selection of healthy cells with large foot area is important to get more fusion events (Figure 3, Methods video S2). Occasionally, some batch of primary cultures show bad secretion performance. Such cultures should be discarded.

Problem 5

Weak imaging signals or high background noise (in STED imaging – day 2–4 section, step 47).

Potential solution

Use higher plasmid concentration for transfection to increase protein expression. We also recommend using the HyD detector with gating for STED signal collection. By gating out the initial signal, background noise can be dramatically reduced. Using the detector filter is also very important to reduce background noise.

RESOURCE AVAILABILITY

Lead contact

Further information and requests for resources and reagents should be directed to and will be fulfilled by the lead contact, Ling-Gang Wu (wul@ninds.nih.gov).

Materials availability

This study did not generate new unique reagents.

Data and code availability

All data reported in this paper will be shared by corresponding authors upon request.

This paper does not report original code.

Any additional information required to reanalyze the data reported in this paper is available from the corresponding author upon request.

SUPPLEMENTAL INFORMATION

Supplemental information can be found online at https://doi.org/10.1016/j.xpro.2022.101404.

ACKNOWLEDGMENTS

We thank Nicholas Cordero for helpful comments on the manuscript. This work was supported by NINDS Intramural Research Program (ZIA NS003009-16 and ZIA NS003105-11).

AUTHOR CONTRIBUTIONS

Conceptualization, X.G., S.H., and L.W.; Methodology, X.G., S.H., L.W., G.A., and W.S.; Investigation, X.G., S.H., L.W., G.A., W.S., and X.W.; Writing - Original Draft, X.G. and S.H.; Writing – Review & Editing, S.H., L.W., G.A., W.S., X.W., and L.G.; Funding Acquisition, L.G.; Supervision, S.H. and L.G.

DECLARATION OF INTERESTS

The authors declare no competing interests.

REFERENCES

Abbineni, P.S., Axelrod, D., and Holz, R.W. (2018). Visualization of expanding fusion pores in secretory cells. J. Gen. Physiol. *150*, 1640–1646. https://doi.org/10.1085/jgp.201812186.

Albillos, A., Dernick, G., Horstmann, H., Almers, W., Alvarez de Toledo, G., and Lindau, M. (1997). The exocytotic event in chromaffin cells revealed by patch amperometry. Nature *389*, 509–512. https://doi.org/10.1038/39081.

Anantharam, A., Bittner, M.A., Aikman, R.L., Stuenkel, E.L., Schmid, S.L., Axelrod, D., and Holz, R.W. (2011). A new role for the dynamin GTPase in the regulation of fusion pore expansion. Mol. Biol. Cell *22*, 1907–1918. https://doi.org/10.1091/mbc.E11-02-0101.

Betz, W.J., Mao, F., and Bewick, G.S. (1992). Activity-dependent fluorescent staining and destaining of living vertebrate motor nerve terminals. J. Neurosci. *12*, 363–375. https://doi.org/10.1523/jneurosci.12-02-00363.1992.

Bhat, P., and Thorn, P. (2009). Myosin 2 maintains an open exocytic fusion pore in secretory epithelial cells. Mol. Biol. Cell *20*, 1795–1803. https://doi.org/10.1091/mbc.e08-10-1048.

Ceccarelli, B., Hurlbut, W.P., and Mauro, A. (1972). Depletion of vesicles from frog neuromuscular junctions by prolonged tetanic stimulation. J. Cell Biol. *54*, 30–38. https://doi.org/10.1083/jcb.54.1.30.

Chiang, H.C., Shin, W., Zhao, W.D., Hamid, E., Sheng, J., Baydyuk, M., Wen, P.J., Jin, A., Momboisse, F., and Wu, L.G. (2014). Post-fusion structural changes and their roles in exocytosis and endocytosis of dense-core vesicles. Nat. Commun. *5*, 3356. https://doi.org/10.1038/ncomms4356.

Gan, Q., and Watanabe, S. (2018). Synaptic vesicle endocytosis in different model systems. Front. Cell Neurosci. *12*, 171. https://doi.org/10.3389/fncel.2018.00171.

Ge, L., Shin, W., and Wu, L.-G. (2021). Visualizing sequential compound fusion and kiss-and-run in live excitable cells. Preprint at bioRxiv. https://doi.org/10.1101/2021.06.21.449230.

He, L., Wu, X.S., Mohan, R., and Wu, L.G. (2006). Two modes of fusion pore opening revealed by cell-attached recordings at a synapse. Nature *444*, 102–105. https://doi.org/10.1038/nature05250.

He, L., Xue, L., Xu, J., McNeil, B.D., Bai, L., Melicoff, E., Adachi, R., and Wu, L.G. (2009). Compound vesicle fusion increases quantal size and potentiates synaptic transmission. Nature *459*, 93–97. https://doi.org/10.1038/nature07860.

Heuser, J.E., and Reese, T.S. (1973). Evidence for recycling of synaptic vesicle membrane during transmitter release at the frog neuromuscular junction. J. Cell Biol. *57*, 315–344. https://doi.org/10.1083/jcb.57.2.315.

Heuser, J.E., and Reese, T.S. (1981). Structural changes after transmitter release at the frog neuromuscular junction. J. Cell Biol. *88*, 564–580. https://doi.org/10.1083/jcb.88.3.564.

Jackson, M.B., and Chapman, E.R. (2008). The fusion pores of Ca2+ -triggered exocytosis. Nat. Struct. Mol. Biol. *15*, 684–689. https://doi.org/10.1038/nsmb.1449.

Kavalali, E.T., and Jorgensen, E.M. (2014). Visualizing presynaptic function. Nat. Neurosci. *17*, 10–16. https://doi.org/10.1038/nn.3578.

Klyachko, V.A., and Jackson, M.B. (2002). Capacitance steps and fusion pores of small and large-dense-core vesicles in nerve terminals. Nature *418*, 89–92. https://doi.org/10.1038/nature00852.

Kononenko, N.L., and Haucke, V. (2015). Molecular mechanisms of presynaptic membrane retrieval and synaptic vesicle reformation. Neuron *85*, 484–496. https://doi.org/10.1016/j.neuron.2014.12.016.

Kononenko, N.L., Puchkov, D., Classen, G.A., Walter, A.M., Pechstein, A., Sawade, L., Kaempf, N., Trimbuch, T., Lorenz, D., Rosenmund, C., et al. (2014). Clathrin/AP-2 mediate synaptic vesicle reformation from endosome-like vacuoles but are not essential for membrane retrieval at central synapses. Neuron *82*, 981–988. https://doi.org/10.1016/j.neuron.2014.05.007.

Miller, T.M., and Heuser, J.E. (1984). Endocytosis of synaptic vesicle membrane at the frog neuromuscular junction. J. Cell Biol. *98*, 685–698. https://doi.org/10.1083/jcb.98.2.685.

Neher, E., and Marty, A. (1982). Discrete changes of cell membrane capacitance observed under conditions of enhanced secretion in bovine adrenal chromaffin cells. Proc. Natl. Acad. Sci. U S A *79*, 6712–6716. https://doi.org/10.1073/pnas.79.21.6712.

Sankaranarayanan, S., and Ryan, T.A. (2000). Real-time measurements of vesicle-SNARE recycling in synapses of the central nervous system. Nat. Cell Biol. *2*, 197–204. https://doi.org/10.1038/35008615.

Sharma, S., and Lindau, M. (2018). The fusion pore, 60 years after the first cartoon. FEBS Lett. *592*,

3542–3562. https://doi.org/10.1002/1873-3468.13160.

Shin, W., Arpino, G., Thiyagarajan, S., Su, R., Ge, L., McDargh, Z., Guo, X., Wei, L., Shupliakov, O., Jin, A., et al. (2020). Vesicle shrinking and enlargement play opposing roles in the release of exocytotic contents. Cell Rep. *30*, 421–431.e7. https://doi.org/10.1016/j.celrep.2019.12.044.

Shin, W., Ge, L., Arpino, G., Villarreal, S.A., Hamid, E., Liu, H., Zhao, W.D., Wen, P.J., Chiang, H.C., and Wu, L.G. (2018). Visualization of membrane pore in live cells reveals a dynamic-pore theory governing fusion and endocytosis. Cell *173*, 934–945.e12. https://doi.org/10.1016/j.cell.2018.02.062.

Shin, W., Wei, L., Arpino, G., Ge, L., Guo, X., Chan, C.Y., Hamid, E., Shupliakov, O., Bleck, C.K.E., and Wu, L.G. (2021). Preformed Omega-profile closure and kiss-and-run mediate endocytosis and diverse endocytic modes in neuroendocrine chromaffin cells. Neuron *109*, 3119–3134.e5. https://doi.org/10.1016/j.neuron.2021.07.019.

Sun, J.Y., and Wu, L.G. (2001). Fast kinetics of exocytosis revealed by simultaneous measurements of presynaptic capacitance and postsynaptic currents at a central synapse. Neuron *30*, 171–182. https://doi.org/10.1016/s0896-6273(01)00271-9.

Sun, J.Y., Wu, X.S., and Wu, L.G. (2002). Single and multiple vesicle fusion induce different rates of endocytosis at a central synapse. Nature *417*, 555–559. https://doi.org/10.1038/417555a.

Taraska, J.W., Perrais, D., Ohara-Imaizumi, M., Nagamatsu, S., and Almers, W. (2003). Secretory granules are recaptured largely intact after stimulated exocytosis in cultured endocrine cells. Proc. Natl. Acad. Sci. U S A *100*, 2070–2075. https://doi.org/10.1073/pnas.0337526100.

Von Gersdorff, H., and Mathews, G. (1994). Dynamics of synaptic vesicle fusion and membrane retrieval in synaptic terminals. Nature *367*, 735–739. https://doi.org/10.1038/367735a0.

Watanabe, S., Rost, B.R., Camacho-Perez, M., Davis, M.W., Sohl-Kielczynski, B., Rosenmund, C., and Jorgensen, E.M. (2013). Ultrafast endocytosis at mouse hippocampal synapses. Nature *504*, 242–247. https://doi.org/10.1038/nature12809.

Wen, P.J., Grenklo, S., Arpino, G., Tan, X., Liao, H.S., Heureaux, J., Peng, S.Y., Chiang, H.C., Hamid, E., Zhao, W.D., et al. (2016). Actin dynamics provides membrane tension to merge fusing vesicles into the plasma membrane. Nat. Commun. *7*, 12604. https://doi.org/10.1038/ncomms12604.

Wightman, R.M., Jankowski, J.A., Kennedy, R.T., Kawagoe, K.T., Schroeder, T.J., Leszczyszyn, D.J., Near, J.A., Diliberto, E.J., Jr., and Viveros, O.H. (1991). Temporally resolved catecholamine spikes correspond to single vesicle release from individual chromaffin cells. Proc. Natl. Acad. Sci. U S A *88*, 10754–10758. https://doi.org/10.1073/pnas.88.23.10754.

Wu, L.G., Hamid, E., Shin, W., and Chiang, H.C. (2014a). Exocytosis and endocytosis: modes, functions, and coupling mechanisms. Annu. Rev. Physiol. *76*, 301–331. https://doi.org/10.1146/annurev-physiol-021113-170305.

Wu, X.S., Lee, S.H., Sheng, J., Zhang, Z., Zhao, W.D., Wang, D., Jin, Y., Charnay, P., Ervasti, J.M., and Wu, L.G. (2016). Actin is crucial for all kinetically distinguishable forms of endocytosis at synapses. Neuron *92*, 1020–1035. https://doi.org/10.1016/j.neuron.2016.10.014.

Wu, Y., O'Toole, E.T., Girard, M., Ritter, B., Messa, M., Liu, X., McPherson, P.S., Ferguson, S.M., and De Camilli, P. (2014b). A dynamin 1-dynamin 3- and clathrin-independent pathway of synaptic vesicle recycling mediated by bulk endocytosis. Elife *3*, e01621. https://doi.org/10.7554/eLife.01621.

Zhang, Q., Li, Y., and Tsien, R.W. (2009). The dynamic control of kiss-and-run and vesicular reuse probed with single nanoparticles. Science *323*, 1448–1453. https://doi.org/10.1126/science.1167373.

Zhao, W.D., Hamid, E., Shin, W., Wen, P.J., Krystofiak, E.S., Villarreal, S.A., Chiang, H.C., Kachar, B., and Wu, L.G. (2016). Hemi-fused structure mediates and controls fusion and fission in live cells. Nature *534*, 548–552. https://doi.org/10.1038/nature18598.